

國立台灣大學生命科學院生命科學系研究所碩士論文



Department of Life Science

National Taiwan University

Master Thesis

活化素/轉化生長因子  $\beta$  於瓢蟲傷口癒合與早期頭部再生  
之研究

Characterization of Activin/TGF- $\beta$  Signaling in the Wound  
Healing and Early Anterior Regeneration of *Aeolosoma viride*

侯蔡涵

Fen-Han Hou

指導教授: 陳俊宏 博士

Jiun-Hong Chen, Ph.D

中華民國 103 年八月

August 2014

國立臺灣大學碩士學位論文  
口試委員會審定書

活化素/轉化生長因子 $\beta$ 於瓢蟲傷口癒合與早期頭部再生之研究

Characterization of Activin/TGF- $\beta$  Signaling in  
the Wound Healing and Early Anterior  
Regeneration of *Aeolosoma viride*

本論文係侯葉涵君 (R01B41033) 在國立臺灣大學生命科學學系、所完成之碩士學位論文，於民國 103 年 7 月 16 日承下列考試委員審查通過及口試及格，特此證明

口試委員：

陳俊彥

(簽名)

(指導教授)

李淑慧

蔡心妤

吳豐翰

生命科學系 系主任

吳益群


(簽名)

## 誌謝

終於順利完成這篇論文了! 整個過程中，我學到最多的就是面對問題、解決問題的能力，而我最大的收穫，就是完成了一件對得起自己的科學研究。回顧兩年的碩士生涯，中間其實遭遇了許多挫折，一開始還因為 DATA 做不太出來，差一點因此而讓我失去研究生物的熱忱；然而，在老師、同學、家人不斷的鼓勵之下，我慢慢能步上軌道，並找回自己讀生命科學的初衷---探索生命現象的奧妙，因而讓我最終得以將論文完成。

首先我要感謝的是我的指導教授，陳俊宏老師。老師對於基礎觀念的要求，是影響我最深的一項因素，也是每個科學人應具備的基礎核心價值。特別是老師常強調的”邏輯思考”一定會謹記在心。再來，我的實驗室夥伴們，平時參與我很多實驗上的討論，也幫助我很多很多。感謝政儀和易澤在我大三剛進實驗室時教了我很多實驗上的觀念，生活上也常從他們那得到很多資訊。感謝謝育，該說是學長還是哥哥呢？我們實在太像了，應該是實驗室最吵的兩個人吧。感謝斐曼姐姐，在實驗上給了我很多幫助!巧坪姐姐，感謝你陪我吵鬧還要常聽我講些五四三，實驗加油！在實驗室大家總是開開心心、打打鬧鬧的邊聊天聽音樂做實驗也讓我在實驗也能有很多樂趣。當然，大學高中時期的好朋友們，在我實驗遇到瓶頸時，陪我散心出遊，是我心靈最佳的調適劑。還要特別感謝在論文、實驗還有生活中幫助我很多的亞軒。沒有你，我大學跟碩士都無法順利完成吧。總是督促我讀書、想實驗、做實驗等等太多太多了。最後，非常感謝我的家人，一路扶持我讓我念書成長。對於我的研究一竅不通的他們很努力的聽我說、替我擔心，是我一直以來最大的後盾!

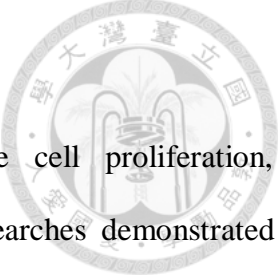
## 中文摘要



活化素(activin)屬於轉化生長因子- $\beta$  (Transforming Growth Factor- $\beta$ )，已知與傷口癒合、發炎反應、細胞分裂及細胞凋亡等有密切關係。過去的研究發現，activin 在老鼠的傷口癒合和斑馬魚的尾鰭再生都扮演著重要的腳色，當 activin 被抑制的時候，老鼠的傷口無法正常的癒合，還有斑馬魚的尾鰭也無法再生。再者，近期研究發現活化素的拮抗分子 follistatin 在渦蟲再生過程中的角色非常重要，因此，本研究想確認 activin 在無脊椎動物中對於再生的重要性。我們選用的模式動物為瓢體蟲 *Aeolosoma viride*，牠是一種水生的環節動物，能在五天再生完成失去的頭部。本篇研究中發現，在 *A. viride* 頭部再生過程中，activin 會大量的表現，activin receptor 會集中表現在 *A. viride* 傷口的位置。接著，以 activin/TGF- $\beta$  的抑制劑 SB505124 處理再生中的 *A. viride* 時，傷口癒合無法正常進行，且再生會被抑制。綜合以上實驗結果，我們推測 activin/TGF- $\beta$  在 *A. viride* 中可能透過傷口表皮癒合來影響再生。

關鍵詞: 再生、傷口癒合、活化素、屬於轉化生長因子- $\beta$ 、瓢體蟲

## Abstract



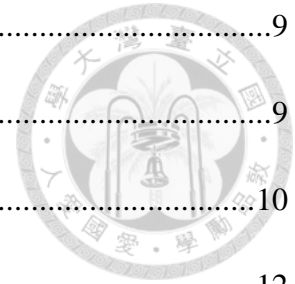
Activin, a TGF $\beta$  superfamily protein, is known to regulate cell proliferation, inflammation, apoptosis, regeneration, and wound healing. Previous researches demonstrated that activin is necessary for wound healing in mice and fin regeneration in zebrafish. Recently, follistatin has been linked to regeneration in planarians. In this research, we investigated the roles of activin in the wound healing of a small fresh water annelid, *Aeolosoma viride*. *A. viride* can fully regenerate the head within 5 days after amputation. The results showed *activin* expression is upregulated during regeneration and *activin receptor* is densely expressed at the wound site and the blastema. Furthermore, *A. viride* treated with a chemical inhibitor of activin/TGF- $\beta$ , SB 505124, obviously inhibited wound healing and impaired regeneration. Therefore, we infer that activin/TGF- $\beta$  signaling might mediate wound healing to affect anterior regeneration in *A. viride*.

Keyword: Activin, TGF- $\beta$ , regeneration, *Aeolosoma viride*, wound healing

# Contents

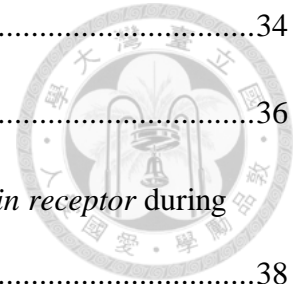


口試委員會審定書.....	i
誌謝.....	ii
中文摘要.....	iii
Abstract.....	iv
Introduction.....	1
Regeneration.....	1
Activin/TGF- $\beta$ Signaling.....	2
Activin/TGF- $\beta$ Signaling and Regeneration.....	3
<i>Aeolosoma viride</i> and Regeneration Research.....	4
Aim.....	5
Materials and Methods.....	6
<i>Aeolosoma viride</i> .....	6
Irradiation.....	6
RNA Extraction.....	6
Reverse Transcription.....	7
Gene Cloning.....	7
Synthesis of DIG-labeled Probes.....	8
In situ hybridization.....	8



Quantitative real-time PCR.....	9
Western Blot.....	9
Immunofluorescence .....	10
Results .....	12
Regeneration of <i>Aeolosoma viride</i> .....	12
Sequences of <i>Avi-activin</i> , <i>Avi-follistatin</i> and <i>Avi-activin receptor</i> .....	12
Activin/TGF- $\beta$ expression profiles during early anterior regeneration.....	13
Activin/TGF- $\beta$ expression in the epithelium of <i>A. viride</i> .....	13
Inhibition of activin/TGF- $\beta$ signaling impairs regeneration.....	14
Inhibition of activin/TGF- $\beta$ signaling disables wound healing .....	16
Discussion.....	17
References .....	21
Tables, Images and Figures .....	27
Table 1. Primers Used for cDNA Identification .....	27
Table 2. Primers Used for qRT-PCR Identification .....	28
Image 1. Map of primers and probes on complete <i>Avi-activin</i> sequence. ....	28
Image 2. Map of primers and probes on complete <i>Avi-follistatin</i> sequence.....	28
Image 3. Map of primers and probes on complete <i>Avi-activin receptor</i> sequence. ....	29
Figure 1. <i>Aeolosoma viride</i> .....	30
Figure 2. Sequence of <i>Avi-activin</i> . .....	32

Figure 3. Sequence of <i>Avi-follistatin</i> . .....	34
Figure 4. Sequence of <i>Avi-activin receptor</i> . .....	36
Figure 5. Expression profiles of <i>Avi-activin</i> , <i>Avi-follistatin</i> and <i>Avi-activin receptor</i> during early regeneration. ....	38
Figure 6. Expression patterns of <i>Avi-activin</i> , <i>Avi-follistatin</i> and <i>Avi-activin receptor</i> . ....	39
Figure 7. Immunohistochemistry of Activin in intact and regenerating <i>A. viride</i> . (A) .....	40
Figure 8. Effects of SB-505124 treatment on the regeneration of <i>A. viride</i> . .....	41
Figure 9. Cell proliferation in the regenerating tissue of <i>A. viride</i> with or without SB505124 treatment. ....	43
Figure 10. Effects of SB505124 treatment on wound closure. ....	45
Figure 11. Radiation effects on wound closure in <i>A. viride</i> . .....	46





# Introduction

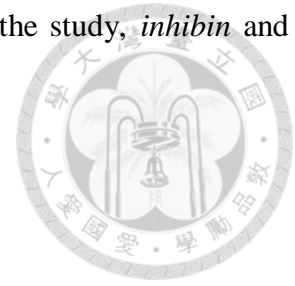


## Regeneration

Regeneration, the ability to restore lost or damaged body structures in animals, is a precisely coordinated process of cell proliferation, cell differentiation, cell migration and tissue remodeling, which are modulated by extensive regulations of genes, signaling molecules, and cell-cell interactions (King and Newmark, 2012). The extent of this ability varies greatly between species but is almost observable in all animals (Alvarado, 2000; Bely, 2010). Renowned research models, hydra and planarians, have phenomenal regenerative abilities that allow them to survive and recover from major body loss (Morgan, 1898; Gierer A et al., 1972; Montgomery and Coward, 1974). At a more limited level, zebrafish and amphibians like xenopus and axolotl, are capable of regenerating damaged heart, eyes, skin or entire limbs (Poss et al., 2002; Whitehead et al., 2005; Chablais et al., 2011; McCusker and Gardiner, 2011; Kizil et al., 2012). Other members of the chordate phylum are merely capable of regeneration. Mammals, for example, can partially regenerate lost digits and recover from acute damage of certain organs (Fernando, 2010; Yu, 2010), but this ability is better observed in infants.

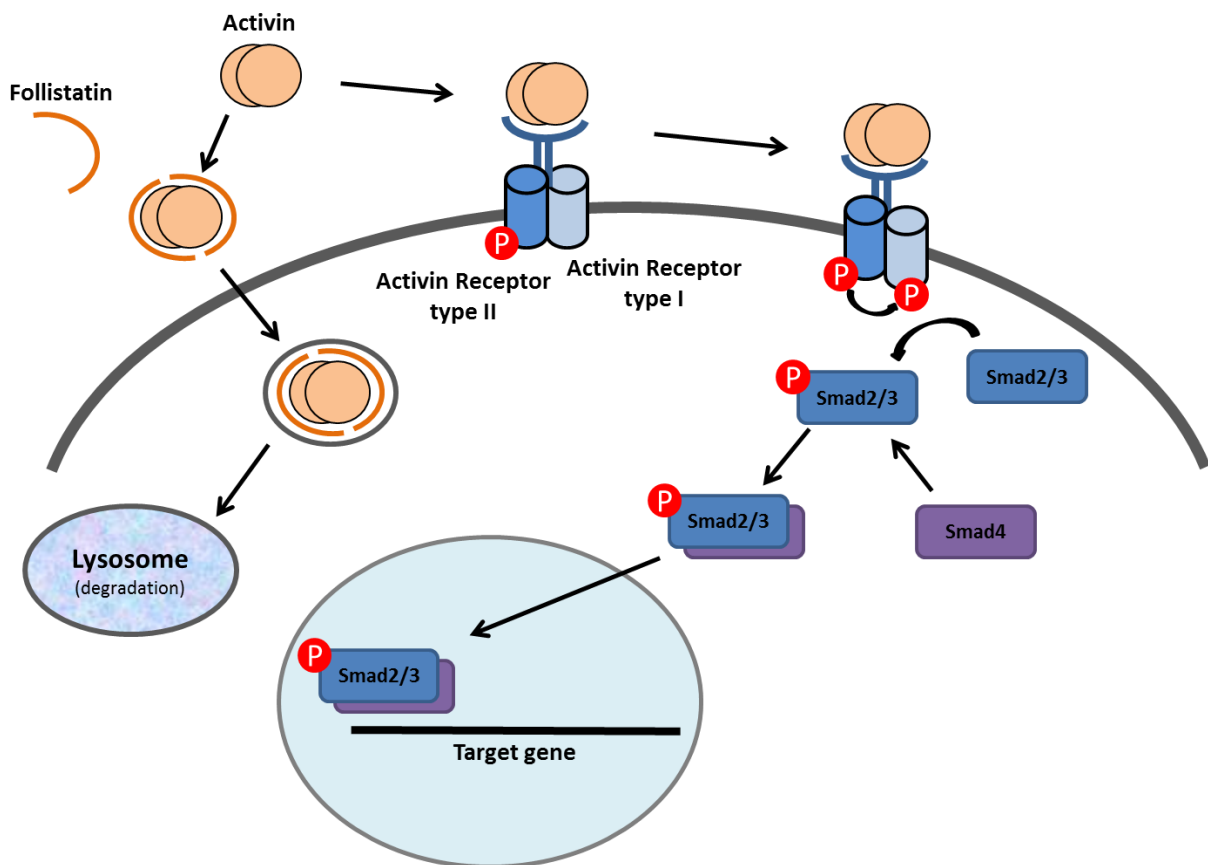
Regeneration research aims to elucidate the differences between regenerative and non-regenerative animals. Studies have identified countless participants that govern different aspects of regeneration, predominantly related to blastema formation and its development. Early wound responses, immediately after injury and leading to blastema formation, remain ambiguous (King and Newmark, 2012). Advancements in technology have made differential analysis of regenerating tissue possible. In 2012, Danielle Wenemoser and colleagues published a microarray analysis of early wound tissue of non-irradiated and irradiated *Schmidtea*

*mediterranea* (Wenemoser et al., 2012). In the list of genes detected in the study, *inhibin* and *follistatin* were identified relatively early in regeneration.



### Activin/TGF- $\beta$ Signaling

Both inhibin and follistatin are antagonists of activin. Inhibin competes with activin for the ligand binding site on the receptor, while follistatin promotes the degradation of activin (Harrison et al., 2005). Activin is a signaling ligand belonging to the transforming growth factor- $\beta$  (TGF- $\beta$ ) superfamily, which includes several secreted dimeric proteins that affect growth and development in a broad range of tissues and organs. After secretion, the ligands bind to their corresponding membrane-bound type-II receptors, which auto-phosphorylates. The



### Activin Signaling

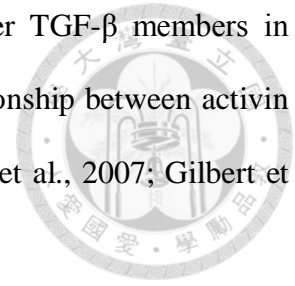
phosphorylated type-II receptor phosphorylates the coupled type-I receptor, also membrane-bound. Subsequently, cytoplasmic Smad proteins are phosphorylated, which interact with co-Smad (Smad4) and ultimately translocate into the nucleus to regulate gene expression (Schmierer and Hill, 2007). Different ligands of TGF- $\beta$  superfamily bind to different receptors and result in the activation of different Smads. Smad1/5/8 are downstream of bone morphogenic proteins (BMPs), and Smad2/3 are downstream of activin, nodal and TGF- $\beta$  (Brown et al., 2007).

Following the discovery of TGF- $\beta$  and other related ligands, their diverse functions have been researched broadly across cell types and animal models. BMP and Nodal of the TGF- $\beta$  superfamily have been studied in the embryonic development of fruit fly (Coutelis et al., 2008), leech (Kuo and Weisblat, 2011) and zebrafish (Xu et al., 2014). Activin and TGF- $\beta$  have been shown to affect cell proliferation of cancer cells and immune reactions (Ishisaki et al., 1998; Chen et al., 2002; Antsiferova and Werner, 2012; Togashi et al., 2014).

### **Activin/TGF- $\beta$ Signaling and Regeneration**

Other than cancer and development, activin has been shown to be highly expressed at the wounds of mice (Hübner et al., 1996; Munz et al., 2001, Zhang et al., 2011). Overexpression of activin promotes the rate of wound closure but causes severe scarring (Munz et al., 1999), while overexpression of follistatin delays wound healing but results in smaller scars (Wankell et al., 2001). In 2007, *activin* was expressed at the blastema of regenerating fins of zebrafish, and the treatment with a chemical inhibitor and morpholino knockdown of *activin* both resulted in non-regenerative fins (Jaźwińska et al., 2007). More recently, in leopard gecko, *activin*, in comparison with other TGF- $\beta$  ligands, was shown to be highly expressed in the wound of

regenerating appendages (Gilbert et al., 2013). While the roles of other TGF- $\beta$  members in development are thoroughly studied across the animal kingdom, the relationship between activin and regeneration is better established in the chordate phylum (Jaźwińska et al., 2007; Gilbert et al., 2013).

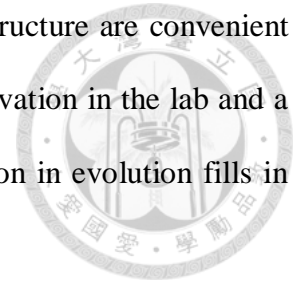


In the field of regeneration, *Schmidtea mediterranea* is the most well-established model. The interactions between activin and regeneration in planarian have recently been studied. In 2012, follistatin has been indicated to be required for the anterior regeneration of the planarian (Roberts-Galbraith, 2013). follistatin was later proven to be related with wound-induced cell proliferation, apoptosis and neoblast response (Gaviño et al., 2013). All researches in the planarian show follistatin expression is essential for anterior regeneration to occur. In other words, activin signaling has to be turned off during anterior regeneration. Interestingly, these results disagree with the observations in the vertebrate regeneration models (Jaźwińska et al., 2007; Gilbert et al., 2013).

### ***Aeolosoma viride* and Regeneration Research**

To further investigate the relationship between activin and regeneration along the path of evolution, we used a novel regeneration model, from the annelid phylum, as they are evolutionarily closer to chordates than flatworms. *Aeolosoma viride* is an aquatic annelid with extraordinary regenerative capacity. It is an opaque worm-like organism with spots of yellow pigment. The organism has around 12 segments, about 2 mm long, but body size varies depending on its reproduction state. The average lifespan of an individual is around 2 months, producing around 10 offsprings. Regeneration requires 5 days to complete, when 5 anterior

segments including head and mouth are amputated. Its size and simple structure are convenient for experimentation on whole organisms. These qualities allow mass cultivation in the lab and a variety of experimental designs and analysis. Most importantly, its position in evolution fills in the enormous gap between platyhelminthes and chordates.

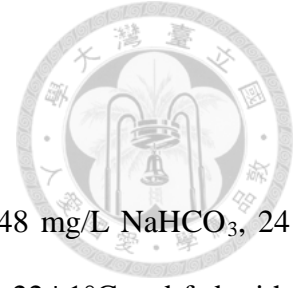


*Aeolosoma viride* is rarely, if not exclusively, used as a regeneration model. Despite the technical difficulties of research on non-model organisms, we have managed to develop a decent system. Previously in our lab, we have identified Wnt pathway genes and confirmed their involvement in the regeneration of *A. viride*. Unlike in the planarian where *wnt* is a posterior polarity specific gene (Petersen and Reddien, 2009), the expression of *wnt* in *A. viride* regeneration is not polarized but blastemal. In addition, *Piwi* and *vasa*, used as neoblast markers in the planarian (Shibata et al., 2010), were observed in the regenerating and reproducing tissue of *A. viride*. The expression of both these genes disappeared after irradiation, supporting their expressions are stem-cell-specific. In earlier researches we have distinguished a few significant characters governing blastema formation and regeneration, but, in search of early response signals, activin/TGF- $\beta$  family members are ideal candidates.

## **Aim**

Given that activin/TGF- $\beta$  signaling plays essential roles in the regeneration of several species, leopard gecko, zebrafish and planarian, this research is aimed to determine the relationship between activin/TGF- $\beta$  signaling and regeneration in *A. viride*.

## Materials and Methods



### *Aeolosoma viride*

*Aeolosoma viride* were cultured in artificial spring water (ASW, 48 mg/L NaHCO<sub>3</sub>, 24 mg/L CaSO<sub>4</sub>·2H<sub>2</sub>O, 30 mg/L MgSO<sub>4</sub>·7H<sub>2</sub>O and 2 mg/L KCl in ddH<sub>2</sub>O) at 22±1°C and fed with ground oat every other day. Subjects were transferred to sterile ASW in preparation for experimentation 4 days in advance. Three days before amputation, worms were synchronized, removing the posterior end, which puts them at the same reproductive state and maximizes the worm's energy expenditure on regeneration. *A. viride* was amputated between the fourth and fifth body segments, maintained in ASW at 23°C and fixed or collected according to succeeding experiments. For fixation, animals were first anesthetized with saturated menthol/ASW solution. Next, saturated menthol/4% paraformaldehyde (PFA) solution was added and the fixed animals were transferred to 4% PFA solution. For RNA samples, *A. viride* was washed several times with sterile ASW and homogenized in Trizol (Invitrogen, Carlsbad, CA) with minimal liquid transfer.

### Irradiation

Intact *A. viride* was placed in a 15mL conical tube, exposed to 90 Gy of  $\gamma$ -irradiation (3 Gy/minute for 30 minutes) and amputated a day after.

### RNA Extraction

Total RNA was extracted using the phenol-chloroform method. Precipitation was done at -20°C overnight and centrifuged at 14,000 rpm for 30 minutes at 4°C. Then, supernatant was

discarded and RNA pellet was washed once with 75% EtOH and centrifuged for 5 minutes. After EtOH was removed, the RNA pellet was allowed to dry. The RNA was then resuspended in diethylpyrocarbonate-deionized water (DEPC-H<sub>2</sub>O) and incubated at 50°C for 10 minutes. The concentration of RNA was tested using NanoDrop™ ND-1000 (Thermo Scientific, Waltham, MA).

### **Reverse Transcription**

Extracted total RNA was reverse-transcribed using SuperScript® III Transcriptase First-Strand Synthesis System (Invitrogen, Carlsbad, CA). Briefly, each reaction composed of 1 µL of 50 µM Oligo-(dT)<sub>18</sub> primer, 1 µL of 10 mM dNTP, 1 µg of RNA and DEPC-H<sub>2</sub>O to a total volume of 10 µL. The reaction was incubated at 65°C for 5 minutes to unwind the secondary structure of RNA and placed on ice immediately for 1 minute. Then, a 10 µL mixture was added; the mixture contains 2 µL of 10X RT buffer, 2 µL of 0.1 M DTT, 4 µL of 25 mM MgCl<sub>2</sub>, 1 µL of RNase OUT™ (Invitrogen, Carlsbad, CA) and 1 µL of SuperScript™ III. This final mixture was incubated at 50°C for 1 hour. The reaction was ceased by increasing the temperature to 70°C for 15 minutes.

### **Gene Cloning**

Partial sequences were obtained from Next Generation Sequencing (NGS) data from Chen's lab and specific primers (shown in Table 1) were designed accordingly. Sequences were confirmed and extended by 3'RACE and 5'RACE methods using primers described in Table 1.

## Synthesis of DIG-labeled Probes

Target sequences were amplified by PCR and inserted into yT&A vector (Yeastern Biotech, Taiwan). Two vectors of opposing orientation were selected for each sequence. DIG-labeled probes were synthesized by in vitro transcription using T7 polymerase (Promega, Madison, WI) and DIG-labeled rNTP (Ambion, Foster, CA). The ssRNA products were precipitated with 1  $\mu$ L of 0.5 M EDTA (pH 8.0), 2.5  $\mu$ L of LiCL and 75.5  $\mu$ L of EtOH at -20°C overnight. Procedure after precipitation is identical to the RNA extraction protocol described earlier. The DIG-labeled probes dissolved in HYB<sup>+</sup> buffer (50% formamide, 5X SSC, 9.2 mM citric acid, 50  $\mu$ g/mL heparin, 0.5 mg/mL yeast tRNA (Sigma, St. Louis, MO) and 0.1% Tween-20 in DEPC-H<sub>2</sub>O) are ready for use.

## In situ hybridization

*A. viride* samples were fixed in 4% PFA at 4°C overnight. After several washes in PBS, samples were treated with 10 mg/mL protease K for 10 minutes and refixed in 4% PFA for 20 minutes. Then the specimens were washed with 0.1% PBST five times, 5 minutes each. Samples were prehybridized in HYB<sup>-</sup> at 65°C for at least 1 hour, and then hybridized at 65°C overnight in HYB<sup>+</sup> with probe concentrations at 1ng/ $\mu$ L. After hybridization, samples were rinsed briefly in HYB<sup>-</sup> and gradually changed to 2xSSCTw, followed by a 5-minute incubation of 2xSSCTw and two 15-minute incubations in 0.2xSSCTw at 65°C. Specimens were then gradually changed to PBS-T at 25°C. Blocking was performed with 5% BSA in 0.1% PBST at 25°C for at least one hour, and then incubated at 4°C overnight in anti-DIG solution at 1:5000. Samples were then washed 10 times with PBS-T at 25°C, 5 minutes each. Prior to staining, samples were washed thrice with staining buffer (100mM Tris-HCl pH 9.5, 50 mM MgCl<sub>2</sub>, 100mM NaCl, 0.1 %



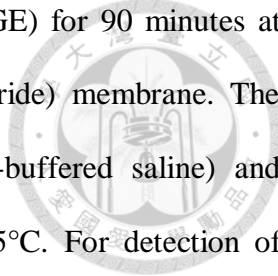
Tween 20), and then stained with staining buffer containing NBT and BCIP at 4°C overnight without agitation and light. The reaction was stopped by adding equal volume of 4% PFA, and incubated at 25°C for 20 minutes. Then, the stained samples were washed several times with PBS-T and gradually dehydrated with methanol. After 3 changes in 100% methanol, samples were kept at -20°C overnight. For microscopy, samples were rehydrated with PBS-T and mounted with 70% glycerol.

### **Quantitative real-time PCR**

Reverse transcription was performed using 500 ng of total RNA from 30 *A. viride* using SuperScript III Reverse Transcriptase, as mentioned previously. Gene expression levels were detected using SYBR® Green Master Mix (Bio-Rad, Hercules, CA) and iCycler iQ Realtime detection system (Bio-Rad, Hercules, CA).

### **Western Blot**

Protein samples were extracted using RIPA buffer with addition of PMSF protease inhibitor right before use. Samples were homogenized with RIPA buffer and centrifuged at 13,000 rpm for 15 minutes at 4°C. The pellet was discarded and supernatant transferred to a new tube for later use. Protein concentration was determined using Bradford reagent (Sigma, St. Louis, MO) and BSA dissolved in ddH<sub>2</sub>O as standard. Samples were adjusted to contain 30 µg at total volume of 20 µL and 4 µL of 6x sample buffer was added. The mixture was boiled in a water bath for 10 minutes to denature the proteins and placed on ice to stabilize its denaturation for another 10 minutes. The samples were then loaded into a polyacrylamide gel and separated



by sodium dodecyl sulfate polyacrylamide gel electrophoresis (SDS-PAGE) for 90 minutes at 4°C. Then proteins were transferred to a PVDF (polyvinylidene difluoride) membrane. The membrane was washed with 0.1% TBST (0.1% TritonX-100 in Tris-buffered saline) and immersed in blocking solution (2.5% BSA in TBST) for an hour at 25°C. For detection of Activin, the membrane was incubated with rabbit-anti-inhibin beta-A (Proteintech, Chicago, IL) at 1:1000 in blocking solution at 4°C overnight. The membrane was then washed with 0.1% TBST several times at 25°C, 10 minutes per wash. Secondary antibody, goat-anti-rabbit IgG HRP (Santa Cruz Biotechnology, Santa Cruz, CA), was diluted at 1:10000 in blocking buffer and incubated with the membrane for 2 hours at 25°C. After 5 10-minute washes with 0.1% TBST, the membrane was rinsed with a mixture of equal parts of Opti-ECL Reagent 1 and Reagent 2. The membrane was visualized by Luminescent Image Analyzer FluorChem M (ProteinSimple, Santa Clara, CA).

### **Immunofluorescence**

Samples were fixed in 4% paraformaldehyde (PFA) at 4°C overnight. Then samples were rinsed with three changes of phosphate buffer saline (PBS) to remove excess PFA and emerged in PBST (0.1% Tween-20 in PBS) for 30 minutes. Samples were submerged in blocking solution (5% BSA in PBST) for 1 hour at 25°C and then incubated in primary antibody solution at 4°C overnight. Primary antibodies were diluted with 5% BSA in PBST as follows: mouse-anti-BrdU (Sigma, St.Louis, MO) at 1:100, rabbit-anti-serotonin (Millipore, Darmstadt, Germany) at 1:500 and rabbit-anti-inhibin beta-A (Proteintech, Chicago, IL) at 1:100. After primary antibody incubation, samples were washed thrice with 0.1% PBST at 25°C, followed by secondary antibody incubation at 25°C for 2 hours, or at 4°C overnight. Secondary antibodies were diluted

with blocking solution at 1:1000. If necessary, samples were then stained with Hoechst 33342 (18ng/ $\mu$ L, Sigma, St. Louis, MO) at 1:1000, PI at 1:1000 or Alexa-633-phalloidin (Invitrogen, Carlsbed, CA) at 1:100. Next, specimens were washed with five changes of 0.1% PBST, 5 minutes each. Then samples were placed on polylysine coated glass slides, immersed in Fluoromount G (Southern Biotech, Birmingham, AL) and sealed.

## Results



### Regeneration of *Aeolosoma viride*

Regeneration in the *Aeolosoma viride* (Figure 1A) requires 5 days, 120 hours, to complete. Immediately after amputation, the wound surface is rough and tissue is exposed to the external environment. (Figure 1B) Within 6 hours, the wound is completely healed (Figure 1C). In the next day, the blastema is formed. The new tissue is low pigmented, as seen above the amputation line (Figure 1D). Between 48 hpa (2 dpa) and 120 hpa (5 dpa), proliferation and differentiation of the blastema takes place until the lost anterior structure is replaced with full function (Figure 1E and 1F).

### Sequences of *Avi-activin*, *Avi-follistatin* and *Avi-activin receptor*

mRNA sequences of *activin* (Figure 2A), *follistatin* (Figure 3A) and *activin receptor* (Figure 4A) were identified and compared with those of other species using NCBI-BLAST. *Avi-activin* has an open reading frame of 510 base pairs, encoding 170 amino acids. The open reading frame of *Avi-follistatin* is 1035 base pairs, encoding 345 amino acids. The current known sequence of *Avi-activin receptor* is 1743 base pairs, encoding a polypeptide chain of 565 amino acids before the first stop codon. NCBI-pBLAST shows conserved domains in each polypeptide chain. Although the predicted *Avi-activin* is only half the size of most known activins, it has a TGF- $\beta$  superfamily conserved domain (Figure 2B). Both *follistatin* and *activin receptor* are about the same size as those in other species, with several sections matching to conserved domains (Figure 3B and 4B). Phylogenetic trees map the amino acid sequences of *activin* (Figure 2C), *follistatin* (Figure 3C) and *activin receptor* (Figure 4C) from *A. viride* with other TGF- $\beta$

superfamily ligands, antagonists and receptors. The results further confirm their identity, grouping activin with other activins, follistatin with other follistatins and identified activin receptor as a type II receptor.



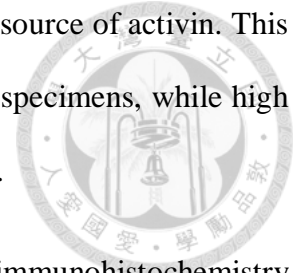
### **Activin/TGF- $\beta$ expression profiles during early anterior regeneration**

In order to determine the connection between activin signaling and regeneration, the mRNA expression levels of *Avi-activin*, *Avi-follistatin* and *Avi-activin receptor* during early regeneration were monitored through qRT-PCR analysis. After amputation, *Avi-activin* increased throughout the first 24 hours and reached its maximum at 24hpa and drops at 48 hpa (Figure 5A). While *Avi-activin* increased from 0 hpa to 24 hpa, *Avi-follistatin*, the antagonist, expression remained stable and increased until 48 hpa (Figure 5B). *Avi-activin receptor*, like *Avi-activin*, also increased throughout the first 24 hpa, but continued to rise and reached its maximal expression at 48 hpa (Figure 5C).

### **Activin/TGF- $\beta$ expression in the epithelium of *A. viride***

To deduce the spatial details of activin/TGF- $\beta$  signaling, *in situ hybridization* (ISH) of *Avi-activin*, *Avi-follistatin* and *Avi-activin receptor* were performed on intact and regenerating organisms. Due to unknown reasons, ISH of *Avi-activin* and *Avi-follistatin* resulted in no observable pattern, mainly because sense and anti-sense samples were indiscriminable (Figure 6A and 6B). However, *in situ hybridization* of *Avi-activin receptor* was successful, and expression was observed on the outermost layer of cells in intact *A. viride*, consistent with the protein expression pattern of activin. This implies that activin/TGF- $\beta$  signaling acts on epithelial

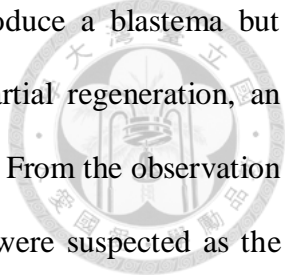
cells, but, without ISH results of *Avi-activin*, it is difficult to conclude the source of activin. This expression pattern of *Avi-activin receptor* was maintained in regenerating specimens, while high expression at the blastema at 24 and 48 hpa was also observed (Figure 6C).



To observe the expression pattern of activin during regeneration, immunohistochemistry was performed on intact and regenerating *A. viride*, which were simultaneously stained with Hoechst, phalloidin and anti-inhibin beta-A. To check the specificity of the anti-inhibin beta antibody, western blotting was performed on total protein sample from intact *A. viride*. The predicted size of activin, from its mRNA sequence, is 19.5 kiloDaltons (kDa), but the single band observed from the immunoblotting is around 16 kDa (Figure 7A). In intact *A. viride*, activin overlaps with a layer of cells lining the external side of the muscle layer, presumably the epithelium (Figure 7B). Throughout early anterior regeneration, activin expression on this outermost layer of cells was maintained without obvious variation in quantity. The expression pattern of the activin protein indicated that activin interacts closely with the epithelium, possibly secreted by or acting on the epithelium. These results fortify the existence of connections between activin signaling, the epithelium and regeneration of *A. viride*.

### **Inhibition of activin/TGF- $\beta$ signaling impairs regeneration**

To further prove the participation of Activin in regeneration, a chemical inhibitor of Activin/TGF- $\beta$  signaling, SB-505124, was used. SB-505124 specifically inhibits Activin/TGF- $\beta$  signaling by prohibiting Smad2/3 phosphorylation through deactivating Activin receptor type I (DaCosta Byfield et al., 2004; Marino et al., 2013). Treatment with 50  $\mu$ M SB-505124 decreased the regenerative abilities of *A. viride*, at 120 hpa (Figure 8A). Individuals incapable of



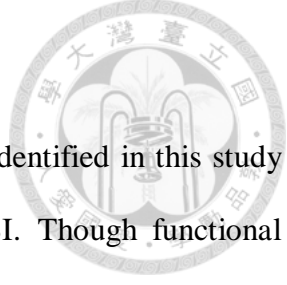
regeneration developed two different levels of severity. One would produce a blastema but remained small at 48 hpa (Figure 8B), while the other type showed partial regeneration, an under-developed head and non-functional mouth-like opening (Figure 8C). From the observation of these two defect types, both cell proliferation and cell differentiation were suspected as the downstream cell processes of Activin/TGF- $\beta$  signaling, linking to regeneration. Due to the lack of a differentiation marker, labelling of the central nervous system with anti-serotonin was performed as an indicator of whether nerve differentiation occurred or not. *A. viridie*, treated with 0.5% DMSO (control) or 50  $\mu$ M SB-505124, were collected 5 dpa and labelled with immunofluorescence. *A. viride* from the control treatment completed regeneration forming a bulged anterior structure with a mouth opening in its center. The central nervous system composed of three vertical lines running down the ventral side, connecting laterally behind the prostomium and formed a circle margining the mouth opening. (Figure 8D) Meanwhile, SB-505124 treated organisms were unable to regenerate, as observed in bright field, formation of an anterior structure with a mouth opening failed. The three lines of nerves did not extend into the new tissue, connect laterally nor surround a mouth opening. In order to examine the effects on cell proliferation, BrdU was incorporated with treatment during regeneration. *Aeolosoma* was treated with 0.5% DMSO or 50  $\mu$ M SB-505124 immediately after amputation. Six hours prior to fixation, *A. viride* was transferred to the medium of previous treatment, but BrdU was added. Cell proliferation was densely shown around the wound and regenerating site of DMSO treated samples, especially obvious at 48 hpa (Figure 9A). On the contrary, SB-505124 treated animals showed little proliferation at the wound site at 48 hpa. Quantification results showed that proliferation was significantly reduced at 48 hpa in SB-505124 treated worms (Figure 9B).

### **Inhibition of activin/TGF- $\beta$ signaling disables wound healing**

Considering the proximity of Activin and the epithelium, Activin/TGF- $\beta$  signaling plausibly affects wound healing in addition to its interference on regeneration. Due to the lack of an epithelial marker, wound was observed by immunofluorescence of Phalloidin and Hoechst. *A. viride* was treated with 0.5% DMSO (control), 50 mM rActivin or 50  $\mu$ M SB-505124. As seen in Figure 10, wound sizes were estimated and plotted against its time after amputation. Control *A. viride* (0.5% DMSO) was able to heal its wound in 6 hours. The wounds of SB-505124 treated worms did not completely close at 6 hpa, wound size at 6 hpa was similar to 0 hpa. rActivin did not have observable effects on wound closure. In other words, inhibition of Activin/TGF- $\beta$  signaling suppressed the wound healing ability of *A. viride*. Given SB-505124 treatment hindered wound closure at 6 hpa but cell proliferation was not significantly affected, whether or not wound closure requires cell proliferation comes into question. To answer the question, the wound healing abilities of non-irradiated and irradiated *Aeolosoma viride* were compared. Wounds at 6 hpa, no matter with or without irradiation, showed no difference in wound size (Figure 11).

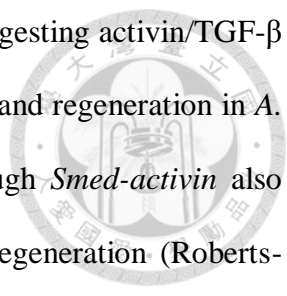


## Discussion



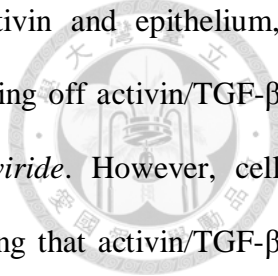
As a non-model organism, sequences from the *Aeolosoma viride* identified in this study were defined based on comparisons with the current database on NCBI. Though functional analysis at the protein level is absent, the genes have been identified as *Avi-activin*, *Avi-follistatin* and *Avi-activin receptor*. The ORF of *Avi-activin* encodes only 170 amino acids, which is about half the size of other organisms. The predicted protein size is 19.5 kDa but western blotting performed with anti-inhibin beta-A detected one band at 16 kDa. Detection of a single band confirms the specificity of this antibody. Although the detected size is smaller than predicted, these results are reasonable because there are many examples of post-translational modifications in the activin of others. In mammals, different types of activin have been identified (de Kretser et al., 2004; Tsuchida et al., 2004) but due to limited research of activin in invertebrates, it was difficult to determine its form. The identified activin receptor has been grouped with other type II receptors, which is a part of its signal transduction but is less ligand specific than type I receptors (Tsuchida et al., 2004). For further clarification, determination of additional TGF- $\beta$  superfamily ligands and receptors, or further analysis at the protein level could be performed.

In order to demonstrate the involvement of *Avi-activin*, *Avi-follistatin* and *Avi-activin receptor* in the regeneration of *A. viride*, their gene expression patterns were studied. Within the first 24 hours after amputation in *A. viride*, the gene expression levels of *Avi-activin* and *Avi-activin receptor* escalated whereas *Avi-follistatin* remained steady, suggesting that activin/TGF- $\beta$  signaling was gradually turned on after amputation. Since *Avi-activin* levels rose and wound tissue increased sensitivity to TGF- $\beta$  signaling by mass expression of *Avi-activin receptor*, while antagonist, *Avi-follistatin*, did not ascend until 48 hpa. Moreover, inhibition of activin/TGF- $\beta$



signaling through SB-505124 treatment hindered regeneration at 5 dpa suggesting activin/TGF- $\beta$  signaling is positively correlated to regeneration. The link between activin and regeneration in *A. viride* opposes the results derived from *Schmidtea mediterranea*. Although *Smed-activin* also gathers at the wounds, knock-down does not cause obvious defects in regeneration (Roberts-Galbraith, 2013). In fact, double knock-down of *Smed-activin* and *Smed-follistatin* rescues *Smed-follistatin* single knock-down phenotypes (Gaviño et. al, 2013). Also in contrast, intermediate cell responses, namely cell proliferation and differentiation of neoblasts, are decreased in *follistatin* knock-down planarian (Gaviño et. al, 2013), but disrupted during activin inhibition in the *A. viride*. Powerful evidence has established that activin signaling has to be turned off during planarian regeneration, but turning off Activin/TGF- $\beta$  signaling impairs regeneration in *A. viride*, and other chordate models.

Distinctions extend to the distribution patterns of activin and activin receptor. In *A. viride*, activin protein and *activin receptor* mRNA were expressed on the outermost layer of cells lining the muscle layer. These signs suggested that activin/TGF- $\beta$  signaling functions on the epithelium. Although lacking mRNA expression patterns of *Avi-activin* and *Avi-follistatin*, it is difficult to identify the source of activin/TGF- $\beta$  signaling. In other words, it is impossible to conclude whether activin is a paracrine agent, released by the muscle and acting on the epithelium, or, an autocrine signal released by the epithelium itself. These expression patterns also differ to those in planarian, where *activin* mRNA is expressed by the gut and *activin receptor* is found in the nervous system (Gaviño et. al, 2013). However, the proximity of activin and epithelium is consistent with studies performed in mice, in which overexpression of either *activin* or *follistatin* altered the morphology of the epithelial tissue (Munz et. al, 1999; Wankell et. al, 2001).



In correspondence to the close relations observed between activin and epithelium, activin/TGF- $\beta$  signaling affects wound closure as well. As expected, turning off activin/TGF- $\beta$  signaling impairs the ability to heal wounds within 6 hours in *A. viride*. However, cell proliferation at 6 hpa was not affected by SB-505124 treatment, suggesting that activin/TGF- $\beta$  signaling influences other cellular processes but cell proliferation, during early regeneration. Since wound closure in *A. viride* does not require cell proliferation, activin/TGF- $\beta$  signaling could be required for epithelial migration or muscle contraction that might contribute to wound closure. Taking into account the different time points of optimal expression, *Avi-activin* at 24 hpa but *Avi-activin receptor* at 48 hpa, we hypothesize that activin has further influences on early regeneration response. Regarding activin's specificity to the epithelium and its concentration in the blastema, activin/TGF- $\beta$  signaling may be crucial to epithelial differentiation.

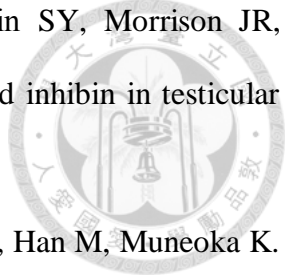
In summary, this study has roughly established that activin/TGF- $\beta$  signaling is upregulated in response to the lost tissue, and is mandatory for regeneration and related processes to occur in the *A. viride*. These results, mostly deduced from chemical treatment, would be better supported with RNAi knockdown experiments, considering possible side-effects from chemical inhibitors, and its toxicity and specificity at high concentrations. Nevertheless, the roles of activin in intact and regenerating *A. viride* are more similar to those observed in chordate models than in planarian. Because activin and other TGF- $\beta$  family members have been known for their broad range of functions and often differ greatly in different contexts, the intermediate cellular processes linking activin and regeneration require further confirmation. Several studies have indicated a positive correlation between activin and cell proliferation (Gilchrist et al., 2006; Zhang et al., 2011; Rodríguez-Martínez et al., 2012; Guzel et al., 2014) while others are negative (Kojima et al., 1993; McCarthy and Bicknell, 1993; Nishihara et al., 1993; Zhang and Ying,

1995; Liu et al., 1996). As well as for cell differentiation, there is controversial data supporting both sides as well (Smith et al., 1990; Green et al., 1992; Davis et al., 2000; Marino et al., 2013). Apoptosis, stem cell regulations and immune responses have also been indicated to be regulated by activin/TGF- $\beta$  signaling (Nishihara et al., 1993; Ishisaki et al., 1998; Chen et al., 2002). Regardless, evidence connecting each phenomenon to activin under regeneration context is relatively limited and need to be studied in the future.

## References



- Alvarado AS. 2000. Regeneration in the metazoans: why does it happen?. *BioEssays* 22(6): 578-590
- Alvarado AS. 2006. Planarian Regeneration: Its End Is Its Beginning. *Cell* 124(2): 241-245
- Antsiferova M and Werner S. 2012. The bright and the dark sides of activin in wound healing and cancer. *J Cell Sci.* 125: 3929-3937
- Bely AE. 2010. Evolutionary Loss of Animal Regeneration: Pattern and Process. *Integr. Comp. Biol.* 50(4): 515-527
- Brown KA, Pietenpol JA, Moses HL. 2007. A Tale of Two Proteins: Differential Roles and Regulation of Smad2 and Smad3 in TGF- $\beta$  Signaling. *J Cell Biochem* 101(1): 9-33
- Chablais F, Veit J, Rainer G, Jaźwińska A. 2011. The zebrafish heart regenerates after cryoinjury-induced myocardial infarction. *BMC Dev Biol* 11:21
- Chen YG, Lui HM, Lin SL, Lee JM, Ying SY. 2002. Regulation of cell proliferation, apoptosis, and carcinogenesis by activin. *Experimental Biology and Medicine.* 227(2): 75-87
- Coutelis JB, Petzoldt AG, Spéder P, Suzanne M, Noselli S. 2008. Left-right asymmetry in *Drosophila*. *Semin Cell Dev Biol.* 19(3): 252-262
- DaCosta Byfield S, Major C, Laping NJ, Roberts AB. 2004. SB-505124 is a selective inhibitor of transforming growth factor-beta type I receptors ALK4, ALK5, and ALK7. *Mol. Pharmacol.* 65(3): 744-752
- Davis AA, Matzuk MM, Reh TA. 2000. Activin A promotes progenitor differentiation into photoreceptors in rodent retina. *Mol Cell Neurosci.* 15(1): 11-21

- 
- de Kretser DM, Buzzard JJ, Okuma Y, O'Connor AE, Hayashi T, Lin SY, Morrison JR, Loveland KL, Hedger MP. 2004. The role of activin, follistatin and inhibin in testicular physiology. *Mol Cell Endocrinol.* 225(1-2): 57-64
- Fernando WA, Leininger E, Simkin J, Li N, Malcom CA, Sathyamoorthi S, Han M, Muneoka K. 2010. Wound healing and blastema formation in regenerating digit tips of adult mice. *Dev Biol* 350(2): 301-310
- Gaviño MA, Wenemoser D, Wang IE, Reddien PW. 2013. Tissue absence initiates regeneration through Follistatin-mediated inhibition of Activin signaling. *eLife* 2: e00247
- Gierer A, Berking A, Bode H, David CN, Flick K, Hansmann G, Schaller H, Trenkner E. 1972. Regeneration of hydra from reaggregated cells. *Nat. New Biol.* 239(91):98–101.
- Gilbert RWD, Vickaryous MK, Vitoria-Petit A. 2013. Characterization of TGF $\beta$  Signaling During Tail Regeneration in the Leopard Gecko (*Eublepharis macularius*). *Dev Dyn* 242(7): 886-896
- Gilchrist RB, Ritter LJ, Myllymaa S, Kaivo-Oja N, Dragovic RA, Hickey TE, Ritvos O, Mottershead DG. 2006. Molecular basis of oocyte-paracrine signaling that promotes granulosa cell proliferation. *J Cell Sci.* 119: 3811-3821
- Goessling W and North TE. 2014. Repairing quite swimmingly: advances in regenerative medicine using zebrafish. *Dis. Model Mech.* 7(7): 769-776
- Green JBA, New HV, Smith JC. 1992. Responses of embryonic xenopus cells to activin and FGF are separated by multiple dose thresholds and correspond to distinct axes of the mesoderm. *Cell.* 71(5): 731-739
- Guzel Y, Nur Sahin G, Sekeroglu M, Deniz A. 2014. Recombinant activin A enhances the growth and survival of isolated preantral follicles cultured three-dimensionally in

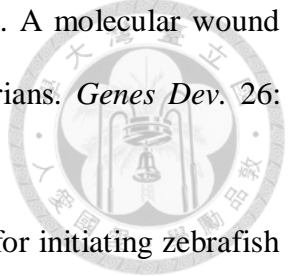
- extracellular basement matrix protein (matrigel) under serum-free conditions. *Gynecol Endocrinol.* 30(5): 388-391
- Harrison CA, Gray PC, Vale WW, Robertson DM. 2005. Antagonists of activin signaling: mechanisms and potential biological applications. *Trends Endocrinol Metab.* 16(2): 73-78
- Hübner G, Hu Q, Smola H, Werner S. 1996. Strong Induction of Activin Expression after Injury Suggests an Important Role of Activin in Wound Repair. *Dev Biol* 173: 490-498
- Ishisaki A, Yamato K, Nakao A, Nonaka K, Ohguchi M, ten Dijke P, Nishihara T. 1998. Smad7 is an activin-inducible inhibitor of activin-induced growth arrest and apoptosis in mouse B cells. *J Biol Chem.* 273(38): 24293-24296
- Jaźwińska A, Badakov R, Keating MT. 2007. Activin- $\beta$ A Signaling Is Required for Zebrafish Fin Regeneration. *Current Biology* 17: 1390-1395
- King RS and Newmark PA. 2012. The cell biology of regeneration. *J Cell Biology* 196(5): 553-562
- Kizil C, Kaslin J, Kroehne V, Brand M. 2012. Adult neurogenesis and brain regeneration in zebrafish. *Dev. Neurobiol* 72: 429-461
- Kojima I, Mogami H, Kawamura N, Yasuda H, Shibata H. 1993. Modulation of growth of vascular smooth muscle cells by activin A. *Experimental Cell Research.* 206(1): 152-156
- Kuo DH, Weisblat DA. 2011. A new molecular logic for BMP-mediated dorsoventral patterning in the leech *Helobdella*. *Curr Biol* 21(15): 1282-1288
- Liu QY, Niranjan B, Gomes P, Gomm JJ, Davies D, Coombes RC, Buluwela L. 1996. Inhibitory effects of activin on the growth and morphogenesis of primary and transformed mammary epithelial cells. *Cancer Research.* 56(5): 1155-1163

- Marino FE, Risbridger G, Gold E. 2013. The therapeutic potential of blocking the activin signalling pathway. *Cytokine Growth Factor Rev.* 24(5): 477-484
- McCarthy SA and Bicknell R. 1993. Inhibition of vascular endothelial cell growth by activin-A. *Journal of Biological Chemistry.* 268(31): 23066-23071
- McCusker C and Gardiner DM. 2011. The axolotl model for regeneration and aging research: a mini-review. *Gerontology* 57: 565-571
- Mochii M, Taniguchi Y, Shikata I. 2007. Tail regeneration in the *Xenopus* tadpole. *Dev Growth Differ.* 49(2): 155-161
- Montgomery JR, Coward SJ. 1974. On the minimal size of a planarian capable of regeneration. *Trans Am Mic Sci* 93: 386–391.
- Morgan T. 1898. Experimental studies of the regeneration of *Planaria maculata*. *Dev Genes Evol* 7: 364–397.
- Munz B, Smola H, Engelhardt F, Bleuel K, Brauchle M, Lein I, Evans LW, Huylebroech D, Balling R, Werner S. 1999. Overexpression of activin A in the skin of transgenic mice reveals new activities of activin in epidermal morphogenesis, dermal fibrosis and wound repair. *The EMBO Journal* 18(19): 5205-5215
- Nishihara T, Okahashi N, Ueda N. 1993. Activin A induces apoptotic cell death. *Biochemical and Biophysical Research Communications.* 197(2): 985-991
- Petersen CP, Reddien PW. 2009. A wound-induced Wnt expression program controls planarian regeneration polarity. *PNAS* 106(40): 17061-17066
- Poss KD, Wilson LG, Keating MT. 2002. Heart regeneration in zebrafish. *Science* 298: 2188-2190





- Roberts-Galbraith RH, Newmark PA. 2013. Follistatin antagonizes Activin signaling and acts with Notum to direct planarian head regeneration. *Proc Natl Acad Sci* 110(4): 1363-1368
- Rodríguez-Martínez G, Molina-Hernández A, Velasco I. 2012. Activin A promotes neuronal differentiation of cerebrocortical neural progenitor cells. *PLoS One*. 7(8): e43797
- Schmierer B and Hill CS. 2007. TGF $\beta$ -SMAD signal transduction: molecular specificity and functional flexibility. *Nat Rev Mol Cell Biol*. 8(12): 970-982
- Shibata N, Rouhana L, Agata K. 2010. Cellular and molecular dissection of pluripotent adult somatic stem cells in planarians. *Dev Growth Differ*. 52(1): 27-41
- Smith JC, Price BMJ, Nimmen KV, Huylebroeck D. 1990. Identification of a potent *Xenopus* mesoderm-inducing factor as a homologue of activin A. *Nature*. 345(6277): 729-731
- Togashi Y, Sakamoto H, Hayashi H, Terashima M, de Velasco MA, Fujita Y, Kodera Y, Sakai K, Tomida S, Kitano M, Ito A, Kudo M, Nishio K. 2014. Homozygous deletion of the activin A receptor, type IB gene is associated with an aggressive cancer phenotype in pancreatic cancer. *Mol Cancer*. 13(1): 126
- Tsuchida K, Nakatani M, Yamakawa N, Hashimoto O, Hasegawa Y, Sugino H. 2004. Activin isoforms signal through type I receptor serine/threonine kinase ALK7. *Mol Cell Endocrinol*. 220(1-2): 59-65
- Vogg MC, Owlarn S, Pérez Rico YA, Xie J, Suzuki Y, Gentile L, Wu W, Bartscherer K. 2014. Stem cell-dependent formation of a functional anterior regeneration pole in planarians requires Zic and Forkhead transcription factors. *Dev. Biol*. 390(2): 136-148
- Wankell M, Munz B, Hübner G, Hans W, Wolf E, Goppelt A, Werner S. 2001. Impaired wound healing in transgenic mice overexpressing the activin antagonist follistatin in the epidermis. *The EMBO Journal* 20(19): 5361-5372

- 
- Wenemoser D, Lapan SW, Wilkinson AW, Bell GW, Reddien PW. 2012. A molecular wound response program associated with regeneration initiation in planarians. *Genes Dev.* 26: 988-1002
- Whitehead GG, Makino S, Lien CL, Keating MT. 2005. fgf20 is essential for initiating zebrafish fin regeneration. *Science* 310: 1957-1960
- Xu PF, Houssin N, Ferri-Lagneau KF, Thisse B, Thisse C. 2014. Construction of a Vertebrate Embryo from Two Opposing Morphogen Gradients. *Science* 344(6179): 87-89
- Yu L, Han M, Yan M, Lee EC, Lee J, Muneoka K. 2010. BMP Signaling Induces Digit Regeneration in Neonatal Mice. *Development.* 137(4): 551-559.
- Zhang M, Liu NY, Wang XE, Chen YH, Li QL, Lu KR, Sun L, Jia Q, Zhang L. 2011. Activin B Promotes Epithelial Wound Healing In Vivo through RhoA-JNK Signaling Pathway. *PLoS ONE* 6(9): e25143
- Zhang Z and Ying SY. 1995. Expression of activins and activin receptors in human retinoblastoma cell line Y-79. *Cancer Letters* 89(2): 207-214

## Tables, Images and Figures

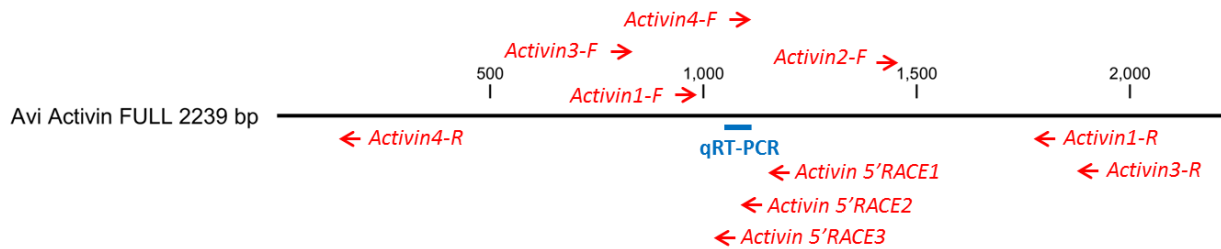


**Table 1. Primers Used for cDNA Identification**

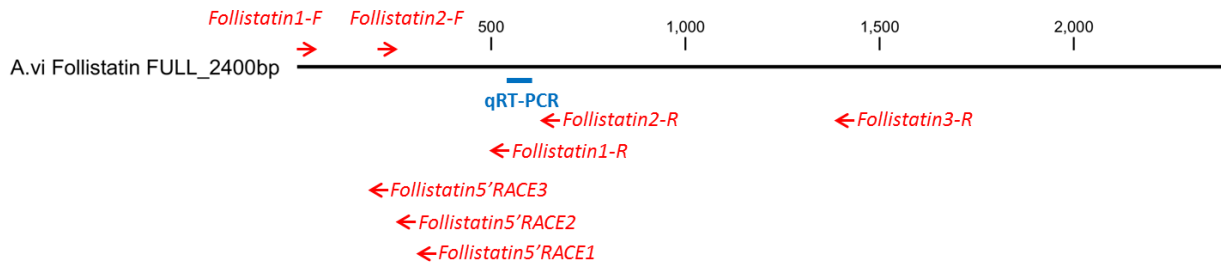
<b>Primer</b>	<b>Sequence</b>
<i>Activin1-F</i>	5-TGCATCGAGAAGCTGTGAGG-3
<i>Activin1-R</i>	5-TCCACGTACGCTGACAATCC-3
<i>Activin2-F</i>	5-ACTTCGCTTGCCTGTGGATT-3
<i>Activin2-R</i>	5-TCGGCTGATTACGAAAGCGA-3
<i>Activin3-F</i>	5-CGACGCGCTTCAAACGACAC-3
<i>Activin3-R</i>	5-ACCGGCTTTTTGGCCAAGCATA-3
<i>Activin4-F</i>	5-GCCCTACAAGCCTCAGCTTT-3
<i>Activin4-R</i>	5-GATGGCGATAAGGCCGGATGA-3
<i>Activin 5'RACE1</i>	5-GGCTAGGTACAGCCACATCGG-3
<i>Activin 5'RACE2</i>	5-GATAGCCGTCGGCGTTCCAG-3
<i>Activin 5'RACE3</i>	5-GGCGTTCCAGAAGAGCACAGA-3
<i>Follistatin1-F</i>	5-GCAAAACAGGATTTACGTGTGC-3
<i>Follistatin1-R</i>	5-GCTCCTCTATGACGGTGCTC-3
<i>Follistatin2-F</i>	5-AAGCGGTGGTTAATGGTGGT-3
<i>Follistatin2-R</i>	5-CATCGCATGATCGTTTGCAT-3
<i>Follistatin3-R</i>	5-AAACGTGCGAGTCCTCCAGC-3
<i>Follistatin 5'RACE1</i>	5-CCTTCGACAGAGCCACACGA-3
<i>Follistatin 5'RACE2</i>	5-CTAGCAGCTGGCATCGACCG-3
<i>Follistatin 5'RACE3</i>	5-ATCGACCGTTGCTGCCATT-3
<i>Activin Receptor1-F</i>	5-AATCGTGGCTGTTGGGCGTT-3
<i>Activin Receptor1-R</i>	5-CACGTTTGGCGGAGCAGACA-3
<i>Activin Receptor2-F</i>	5-ACTGCTATGCATCGTGGCGG-3
<i>Activin Receptor2-R</i>	5-GCGAGCCTCAGGGTCAACAT-3
<i>Activin Receptor3-F</i>	5-TCGCCTCTCAGCCTATTGTG-3

**Table 2. Primers Used for qRT-PCR Identification**

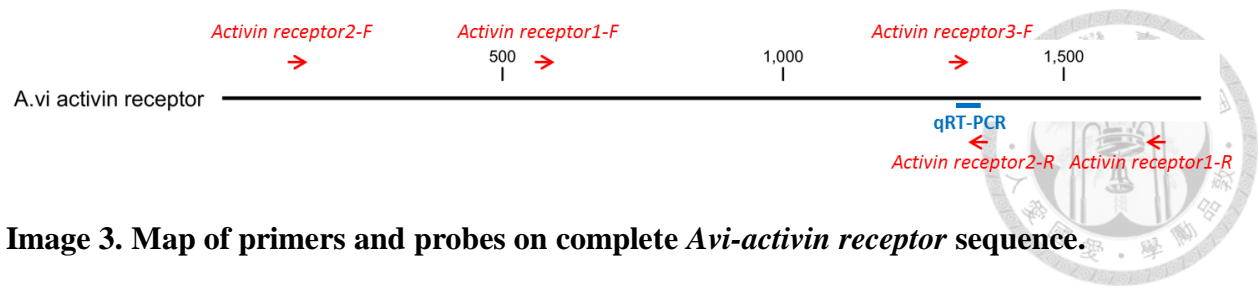
Primer	Forward	Reverse
<i>ActivinRT</i>	5- CATCATGCTGTGCTCCTACTA A-3	5-GCCACATCGGTCAACTATCA-3
<i>FollistatinRT</i>	5- AAAGCGAGCACCGTCATAG-3	5-CGACAATTTGACCGCAACAG-3
<i>Activin Receptor RT</i>	5- GGCCTGTTATTAGAGAGGAA TGG-3	5- CAAGGACACAATAGGCTGAGA G-3



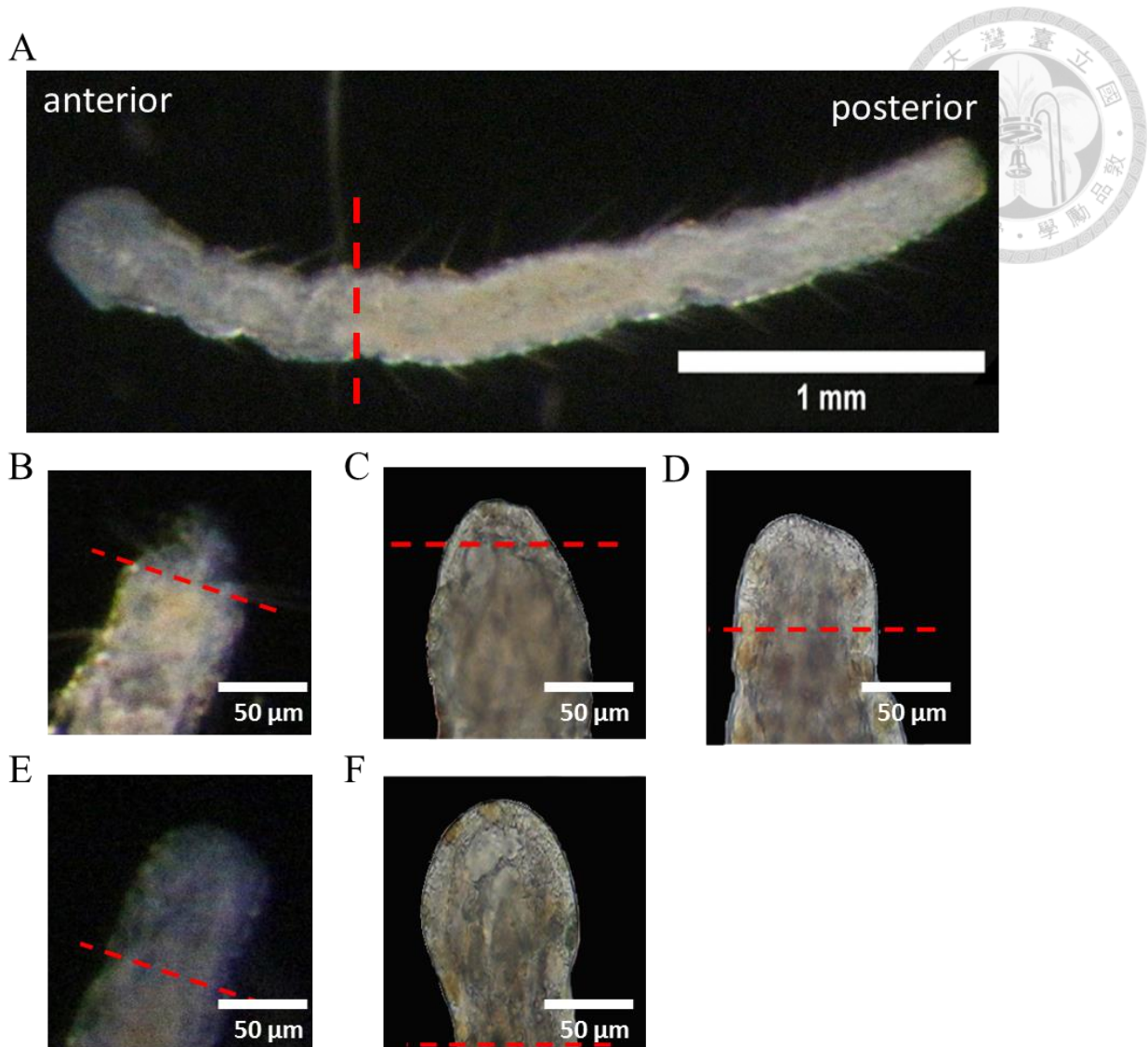
**Image 1. Map of primers and probes on complete *Avi-activin* sequence.**



**Image 2. Map of primers and probes on complete *Avi-follistatin* sequence.**



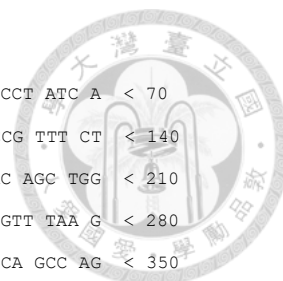
**Image 3. Map of primers and probes on complete *Avi-activin receptor* sequence.**



**Figure 1. *Aeolosoma viride*.** (A) Intact *A. viride* are 2-3 mm long, have a bulged anterior structure with a mouth opening and sexually reproduce in the posterior region. Prior to regeneration studies, samples are amputated between the 4<sup>th</sup> and 5<sup>th</sup> segments, immediately anterior of the stomach, red dashed line. (B) 0 hpa. Edge is rough with exposed tissue. (C) 6 hpa. Wound healing has completed and site of injury is smooth. (D) 24 hpa. The blastema has formed above the amputation line with less pigmentation. (E) 48 hpa. Proliferation of the blastema increases its size. (F) 96 hpa. Differentiation has begun, mouth opening beginning to form. Dashed line: amputation line.

# A

ATC GAG GAG GCT CGG CAT CCT TGA CTA TTC CCA ACT CTT CCC CCA ATC GAA CAT CTA CGA CTC CCT ATC A < 70  
 GT ACG TAA TCA TTT TTT CCC ATC GCT TAC GAA TAT GGC GAT TAC GAT GCA GCA CAG TCA GAT CCG TTT CT < 140  
 A TCA GAT GAT TAT CAG CCG TCA GAT CAT CCG CTT ATC GCC ATC ATG CGA CCT GGC CGA AGA AAC AGC TGG < 210  
 AAG ACG ATG GTG ACA AAA CGA CAG AGA TTG TCA TCT TCG GGA CCG CAG TGC CAT CAA ACG AAT GTT TAA G < 280  
 TG CTG ACC AAA GCG GAG TTG GTG ACA AAA CTG ACA AGA GTG TCT ACT GTT TTC AGT TTG ACG TCA GCC AG < 350  
 C GAT TAA CGG AGA ATC GCA AAA TCA CTT CCG GCC AGC TGT GGC TGT TCA AGC AGG CTG CTT CAT ACC CGT < 420  
 CGC GCA TGC GTG CTC ATC GAG CTA GCG CTG AAA CAG TTG CCC TTT ACG AAA CAA AAA GTT GAC TAC TAC C < 490  
 AT CAT CTA CAA CAA TTT TTA GCT AAT AAA TCA GCC TCT GTG TCG CGT CAA AAA AAT GAT GTA AGC TTT GT < 560  
 T CAT CGT GCC GGT CGC CGA CTA GAC CAG AAA GAT GTA AGT CGT GCG GAT GAC TCG TGG CTT GAA ATG AAC < 630  
 M N  
 TTG TCC CTG GCA TTA AGT TCG TGG CAA CGT GGC AGC AAC GGG AAG AAG GTG CTG CTA ATC CAG TGC AAG A < 700  
 L S L A L S S W Q R G S N G K K V L L I Q C K T  
 CT TGC AAC ACC ACT TTA CGG CCT TTC CTG CGC ACA AAC AGC CCC TAC GAG CCT TAC ATC GTG CTT AAA TT < 770  
 C N T T L R P F L R T N S P Y E P Y I V L K L  
 G GGT CAA CTC ATT CGT ACG ACG CGC TTC AAA CGA CAC GTA GTT GAA TGC AAG GGT TCT CTG AGT CAC TGC < 840  
 G Q L I R T T R F K R H V V E C K G S L S H C  
 TGT CTA AAT CGC CTG TAC GTC AGC TTC TCT GAT TGG GCT CCA AGC ATA CAA CAA CCT GAT GGT TTC TGG G < 910  
 C L N R L Y V S F S D W A P S I Q Q P D G F W A  
 CT AAC TAC TGT CGA GGA AAC TGT CAA GGC CGC CTT CTG CCA GCG CAG AGA CAC AGT ACT CTG ATG ATG CA < 980  
 N Y C R G N C Q G R L L P A Q R H S T L M M H  
 T CGA GAA GCT GTG AGG CGG CAA GAC GAT GTC GAG ATA CCA TCA TGC TGT GCT CCT ACT AAG TAC TCA GCT < 1050  
 R E A V R R Q D D V E I P S C C A P T K Y S A  
 TTA TCT GTG CTC TTC TGG AAC GCC GAC GGC TAT CTG ATT AAG CGT GAC TTG CAA AAC ATG ATA GTT GAC C < 1120  
 L S V L F W N A D G Y L I K R D L Q N M I V D R  
 GA TGT GGC TGT ACC TAG CCT GAT ATC TGT CAT TAT AAC TAT GTG AAG AAT ATG TTT TCA TCC GGT ATC AT < 1190  
 C G C T \*  
 A TTC CTA GGT TTC GTT CCT AGG CTC AAC TTC ACT TGA ATT TAC TGC CAC ATT AAC TGA GCA ATT TTG TTT < 1260  
 GTT TGT TTG GCT GAT CAT TGT GTT TTG TTT GCA ATT TGT TAT TTG CCT TGT TAT AAA TAA AAT TAC TTG T < 1330  
 TA AAC TAT TGT AGT ACA CAG GTG TGA AGT ACA TAC TTA CTT AAT GAA ATA ACT ATA CGA TTA AAT GCA GC < 1400  
 T AAC TCA GTA ACT CTT TCA CTT CGC TTG CCT GTG GAT TAC TTG TAT TAA ATT TAG TAT AAC GAC TAG GCT < 1470  
 AAA TAA AGG AGA GTT AAT AAA ACA GTT TAA TTT ATT TCT ATG CTA GAA CAT TAT TGT ATT GCC TAA TGG T < 1540  
 TA TGA ATA GTA ATT CGG AGT TTT CCT CAA CAA CAA AAC TTG TGA AAA ATT TTT AAG AAT ATT TAT TTC AA < 1610  
 G TAT TTT TAC TGT GTC GAA TTG CAG ACC TAT GTA AAC TCT AAA CTG AAA TTT ATA TAA ATG CAG CTC TTA < 1680  
 TCT GTA TGC ATA TAA ATG TAT TTT GTT ATT TTT CAA GCT ATA GTT GTT ATT AAT TTA GTC GCG TGT ATG T < 1750  
 GT TTA TTG CAC TAT TTT GTA AGT GTC ATA TTT TTC TTA TAC GTG TAT GAA AAT TGA CGA ACT GCG TTT GG < 1820  
 T ACA TAG AGT TGG ATT ATC AGC GTA CGT GGA TCT GCA CTA TAT GCT TGG CCA AAA AGC CGG TGT ACA AGT < 1890  
 AAA AAA CAA GTT TTT ACA ATT ATA TAT GCT GAA ATG ATG TCG ATA TAA GAT TAT AAA AAC TTG TTT AAT A < 1960  
 AC AAG CGC ACA GTT CTT GAC CGT GTG ATA CCA GCT TAA GGT AGA TCT TAT ATT CAC GTA GTA ACA CTG CA < 2030  
 T GTC GTT TTT CAA TGT TTG TCA AAA ATC TAT ACA ACT AGG TGA GAT AGT TGC GCA TTC AAA TAT GTC ATG < 2100  
 TAA TTT GTC ATG TGA TAT GTC ATG TGA TAA GTA ATT GAA AAT TAT CCT TAA TTT ACT GTT TAT ATG TAA G < 2170  
 TA TAT AAT AAA AAT TAA TTA TTT GCG TGA AAA GAA AAA AAA AAA AAA AAA AAA AAA AAA AAA AAA < 2238



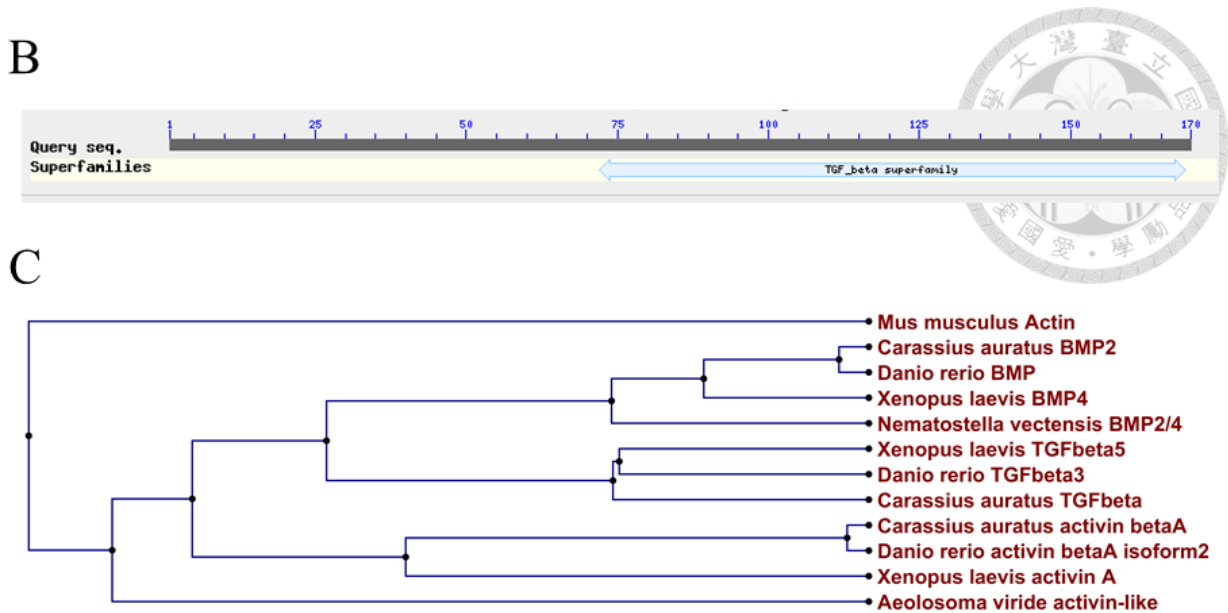
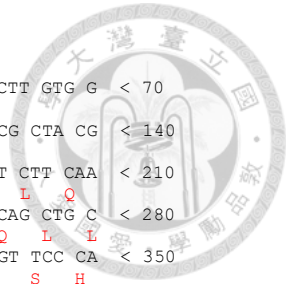


**Figure 2. Sequence of *Avi-activin*.** (A) The full length sequence, from 5'UTR to poly-A tail, is about 2200 base pairs long. The ORF consists of 510 b.p. encoding 170 amino acids with a TGF- $\beta$  superfamily conserved domain (from NCBI) (B). (C) Comparison of the polypeptide sequence derived from *A. viride* with known TGF- $\beta$  family ligands from other species groups it with other Activin proteins. *Danio rerio*: zebrafish. *Carassius auratus*: goldfish. *Xenopus laevis*: African clawed frog. *Mus musculus*: house mice. *Nematostella vectensis*: starlet sea anemone.

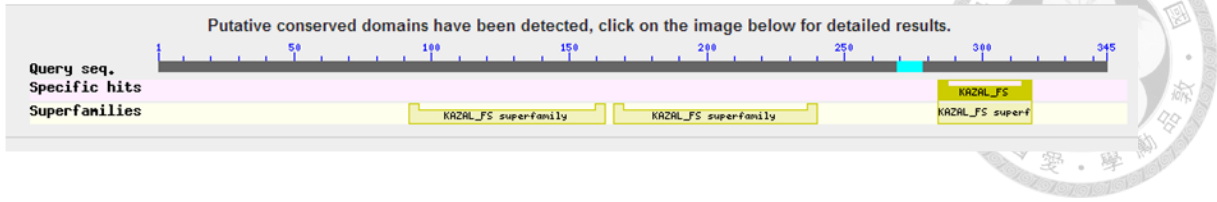


# A

GAT TTC TCG ACG GAT TTA CGT GTG CAT CAT CTT ACT CTA CTC AGC GTG AAT AGA AGA CGT TTT CTT GTG G < 70  
AA TAT CAA TCA TTT AAA AAT ATT CTT TAT ACT ATA ATT TTT TTG TTT TGA ATT TAG TAT CAT ACG CTA CG < 140  
T TTC ATT TGA TAA AAA TCA AGT ACT ATG ATT GAG AGG CAA AAA TTT TTT TTA TTC CTC GCG CTT CTT CAA < 210  
TCT TTT GAA GCG GTG GTT AAT GGT GGT ATA TGT TGG CTA ACA ATG GGC AGC AAC GGT CGA TGC CAG CTG C < 280  
S F E A V V N G G I C W L T M G S N G R C Q L L  
TA GAT CGT GTG GCT CTG TCG AAG GAG GAG TGC TGC CAA ACA GGA GCC GTT AAC GCC GCT TGG AGT TCC CA < 350  
D R V A L S K E E C C Q T G A V N A A W S S H  
C AAT GAG GCT ACT CTC AGG CCG GGT CAG TTC TTT TAC TGG GAG TCG TTT AGT GGC GGA GCG GAC AAG TGC < 420  
N E A T L R P G Q F F Y W E S F S G G A D K C  
GAG CCT TGT CAC GTA AAT TGT GAC CGG GTG TCC TGC TCG GCT GGA AAG AAG TGT GTG ATG CGG GAC AGC A < 490  
E P C H V N C D D R V S C S A G C K K C V M R D S R  
GG CCC CAG TGT GTG TGC TCT CCC GAC TGT TCG CAA AGC GAG CAC CGT CAT AGA GGA GCT CTG TGC GGC AC < 560  
P Q C V C S P D C S Q S E H R H R G A L C G T  
T GAT GGA CGA AAC TAC GAT AAT CAT TGT GCC CTG TTG CGG TCA AAT TGT CGC AAA GAC CAA TAT ACG GAA < 630  
D G R N Y D N H C A L L R S N C R K D Q Y T E  
ATT GAC TAT TTC GGA AAG TGC AAA CGA TCA TGC GAT GAA GTT CAG TGT GCT CGT GGT AAA CAC TGT GTG G < 700  
I D Y F G K C K R S C D E V Q C A R G K H C V V  
TT GAT CAA AAC GCT TTG CCT CAC TGT GTG ATG TGC ACG TCT TTG GCT ACT TGT CAA CGT CTG AAG GGA CC < 770  
D Q N A L P H C V M C T S L A T C Q R L K G P  
G CAC GAA CGT TTA TGT GGC GCT GAT GGC GTT ACG TAC GAG TCA CTT TGT CAT TAT AGG CGT GCG GCC TGT < 840  
H E R L C G A D G V T Y E S L C H Y R R A A C  
ATT GCC GGC AGA GCA ATG AGC ATA GCT TAT ACC GGG GAA TGC AAA GCA TCA GCA ACT TGC GCA GAC ATC A < 910  
I A G R A M S I A Y T G E C K A S A T C A D I T  
CG TGC GGT TCT GGT ATG AAA TGC TTG CTT AAC TCT GTC ACA AAT CGG CCG CAG TGT GTC ACT TGC TCA GC < 980  
C G S G M K C L L N S V T N R P Q C V T C S A  
T ACT ACG TCA TGC ACG GCT GGT CGC AGC GCG GGT CCG GTT TGT GGT ACA GAC GGT CGT ACA TAT GCA AAC < 1050  
T T S C T A G R S A G G P V C G T D G R T Y A N  
TGG TGC ACA TTA CGA GAA GAG GCC TGC CGC AAC GGT TAC GTC ATA GAG ACC CAG CAC TTC GGA GAG TGC G < 1120  
W C T L R E E A C R N G Y V I E T Q H F G E C G  
GG ACA GGC ATA GGT TCC TGG GCT AGC AAC AGT CAA GAA GAT TAT TAT GAC GAC GAT TCC GCA ACT GCG TT < 1190  
T G I G S W A S N S Q E D Y Y D D D S A T A L  
A TTA CGA CGT CGG TAA CGA AGG GCC CCC TAA ACC AGC CAT TTT TGG ATG GAT TCA TAT ATG AAT TAT TGT < 1260  
L R R R \*  
CAT ATA GGA GCG CAG TTT TTA TTT AGC TAT TAA TTC AGA GGA CAG GGT AAT TGT GAC TGT ACT CGT CTG C < 1330  
TA CGT CGT TCG CAC AAC TGT TGT GTA CTA TAT GTG AAG CAT CTC GGT CAG CCT TGC TGG AGG ACT CGC AC < 1400  
G TTT TGT TAT CGT TGC TTG AAG GCC GGA ATA TTC CAG TGG CTG AGA GTT GTT GAA AAA TTG TAC AGC TTA < 1470  
AAT GTT ATT ACA ATA ATG TTA GGA AAT GAC TTT TGT GTT CAC TGT TAG TGT TAT ATT TAT TTT AAA AGT A < 1540  
TT TTA CTC CTT GTA ACA CTT CTT GCA TGA TAT TTC TTA ATG TGT AAT TTA TTT ATT ATT TAT GGC TTC AG < 1610  
G CAG CGA TGT ATT GCT TTA TTT ATT TAA AGA TAG CTT GCA TGC AAG ACT GTT TTT GTG AAA TTA CAG CTT < 1680  
TTT TTG GCT GCA ATT GCA TTT GAA ATT CGT ATT TGT TGC ATA ATT TTT GCG TAA CTT TAG AAT TTT GAA T < 1750  
AT AGG AAA TAA GGC TAA ACC ATG AAA TTT GAA AGA TTG TAC TGC ATT ATA TAT AGG AAA TGT TAA GTT TG < 1820  
C CCG TAC CAA TCA CAG TAT GTC TAG GTA TAC TGT AGT ACT CAT AGT GTA TAT AGT TAC ACC ACT TTT ACG < 1890  
TCA CAT ATT ATT AAA AAA AAG CAA ACT CAA ATG ACA TCC ATA GTG CAA TTT TTG CCA AGT GCC AGT CTT A < 1960  
CA ATG GCT GAT GTC ATT ATC AGT ATT ATA ACA GCT GAT ATC AGC ATT CAG CAG TAA ACC ACA TCA GTA TG < 2030  
A ACT TTT TTA GTT GCA TTG CAC TAA TAT ACA AAT CTC TTA GCA AAC TGT GTT GTG GTA CTG CAT ACT TTA < 2100  
AAT ATC AAC AGA TCT ACA AAA ATG ATT GTC ACT GAT ATG AAG TTG TGA TTT ATT TTA TTT ATT TGT TGT G < 2170  
CA ATC GTT TAC TAA TGG TGT TTA CTT TGA TAG TTT ACT TCC TCT ATT GAT GGT TGT TAT ACA TAC TGC AG < 2240  
T AAA CGT TAA TAT CTA CCT CGA CGG ACA ACC ATT GAG TAT TGA ACT GTT CGT GCT GTG GTA GCT ACT GTT < 2310  
TTG TTA ATC CGA AGG GAA GAA CTA GAA CAT GGC ATG GTG CCG AAT TGT TGC TTT AAT AAA TAG TTC AGC T < 2380  
CT AAA AAA AAA AAA AAA AAA AAA AAA A < 2407



B



C

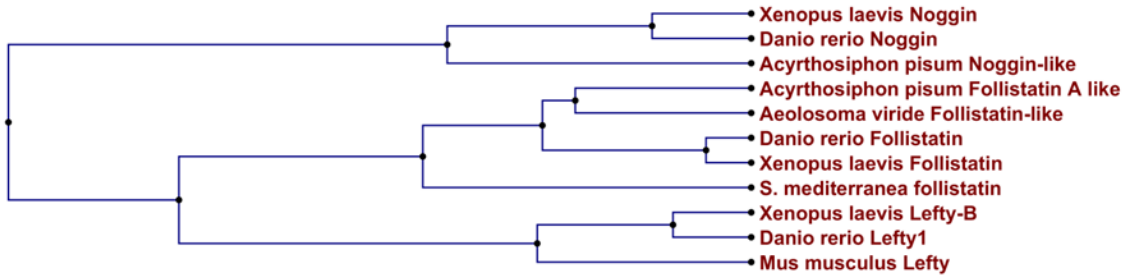


**Figure 3. Sequence of *Avi-follistatin*.** (A) The full length sequence, from 5'UTR to poly-A tail, is about 2400 base pairs long. The ORF consists of 1035 b.p. encoding 345 amino acids with follistatin conserved domain (from NCBI) (B). (C) Based on the phylogenetic tree of TGF- $\beta$  family, follistatin of *A. viride* is closest to other follistatins than other TGF- $\beta$  family antagonists. *Xenopus laevis*: African clawed frog. *Danio rerio*: zebrafish. *Acyrthosiphon pisum*: pea aphid. *S. mediterranea*: planarian. *Mus musculus*: house mice.

# A

GT CGA GTA TGT GAA TAC TAT AAC CAA AAA GAA TGT GAG AGC GAG AAT TGC AGT AAA ATA GAA GAA TGT < 68  
R V C E Y Y N Q K E C E S E N C S K I E E C

CCT GTT GCG GAA GCT GAT AAA CGA TCG CAC TGC TAT GCA TCG TGG CGG AAT GAA ACT GGT AAC ATA AC < 136  
P V A E A D K R S H C Y A S W R N E T G N I T

A ATT ATT ATG CAA GGA TGC TGG CTT GAT CTG CAT GCT TGT TAC GAC TGG ACA GAA TGT GTT GCT CGA T < 204  
I I M Q G C W L D L H A C Y D W T E C V A R S

CA TGG GAC AAA ATA TTA TTC TGC TGC TGT GAC GCA GAC ATG TGT AAT ATT AGG ACA AAC ATT TCA TAT < 272  
W D K I L F C C C D A D M C N I R T N I S Y

ATA CCA TTA CCT GCT ACC GAA ACT TCT GCT GTT GGT ATA CAA GAA ATA AAC TTA TCT GGA GGA TTA TT < 340  
I P L P A T E T S A V G I Q E I N L S G G L F

T TTC TCT TAT GCT TTG TTG CCA CTT GTG GTA CTA TCA TGT ATC TGC GCA ACT TTA TTC TTT ATA TGG C < 408  
F S Y A L L P L V V L S C I C A T L F F I W R

GA CAA TGT CGC CAA CAT GAT TTT CCA AGG GAA CAC TCG TCT CTC ATG GAT CCC TTA ATG CAA CAA GAA < 476  
Q C R Q H D F P R E H S S L M D P L M Q Q E

GAA GCC AAG ATT ATC CAA AAA CCA AAT GCA CAA TTT ACC CAT AAG CTA GAA ATC GTG GCT GTT GGG CG < 544  
E A K I I Q K P N A Q F T H K L E I V A V G R

T TTT GGT TGT GTG TGG AGA GCT AAA CTG CAA ACA CAG CAT GGC TAC AAA GAA GTT GCC CTC AAA ATA A < 612  
F G C V W R A K L Q T Q H G Y K E V A L K I M

TG AAG AGT CAA GAG AGA GCT TCA TGG AGA CGT GAA ATT GAA GTT TAT GAA TTA CCA GGC ATA AAA AAT < 680  
K S Q E R A S W R R E I E V Y E L P G I K N

AAT GAA AAC ATA CTA ACT TTT GAA TCA GCT GAA GAA TAT GCA TCA GAA AAA GAA TTA GAA CTA AGA AT < 748  
N E N I L T F E S A E E Y A S E K E L E L R I

T TTA ACT GAA TTT CAT CGT CGA GGC TCA TTA CAT GAT TTC CTG AAA ATT ACT GAG CTA AGC TGG AAT A < 816  
L T E F H R R G S L H D F L K I T E L S W N N

AT CTG TTA ACT ATT GCG GAA TCA ATG CTA CGT GGC CTG GCA TAT CTT CAT GAA GAA GTG GGA GCA AAA < 884  
L L T I A E S M L R G L A Y L H E E V G A K

CCA GCT ATT GCC CAT CGT GAT TTC AAA AGC AAG AAT GTA ATA TTA AAA GAA GAT TTA ACT GCG TGT AT < 952  
P A I A H R D F K S K N V I L K E D L T A C I

A GGA GAT TTT GGG CTT GCA ATA ATC TTT GAA AAT GGG AAT AAC ATT GGA GAT ATC TAC TCA CAG GTG G < 1020  
G D F G L A I I F E N G N N I G D I Y S Q V G

GC ACT CAT CGT TAC ATG GCT CCA GAA ATA CTT GAT GGG GCA ATG TGT TTT AAC CGT GAT GCA TTT CTA < 1088  
T H R Y M A P E I L D G A M C F N R D A F L

CGT GTT GAT ATG TAC GCA TGT GCT TTG GTT CTT TGG GAA ATG ACT AAT CGT TGC ACT GTT TTA GGA AC < 1156  
R V D M Y A C A L V L W E M T N R C T V L G T

T TGT GGT GTG TAT AAA CTT CCA TAC GAA GAG TTG GTT GGT CTC AAT CCC ACT GTT CAA GCT TTG AAT G < 1224  
C G V Y K L P Y E E L V G L N P T V Q A L N E

AA GTT GTA ACT AAA AAG GGT CGC AGG CCT GTT ATT AGA GAG GAA TGG AGG AAA CAT GAG GGA TTG CAA < 1292  
V V T K K G R R P V I R E E W R K H E G L Q

GTG CTG GCT GAA ACT TTA GAT GAA TGT TGG GAT GTT GAC CCT GAG GCT CGC CTC TCA GCC TAT TGT GT < 1360  
V L A E T L D E C W D V D P E A R L S A Y C V

C CTT GAA CGT CTT TGT GAG CTG AAA TCA AAG TCA TGC TCT ATG TCG TCT CTA TCT GCA AAT GGT GAC A < 1428  
L E R L C E L K S K S C S M S S L S A N G D K

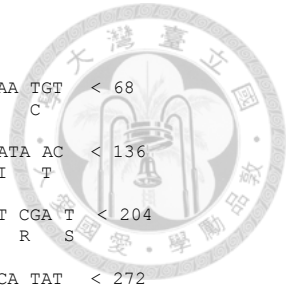
AG GAT AGC GCT TGC TCT GTA TCT TTC CCT GGT ATT ACC ATA GAT TCA ACA GAT GAC GAA CAT AAG CCA < 1496  
D S A C S V S F P G I T I D S T D D E H K P

GCT ACT GGG GAA ACG TCC CTT AAC ACT GTG GAT TTG GTG ACA TAT CAC AGT GAA GAT AGT GAA GAT AC < 1564  
A T G E T S L N T V D L V T Y H S E D S E D T

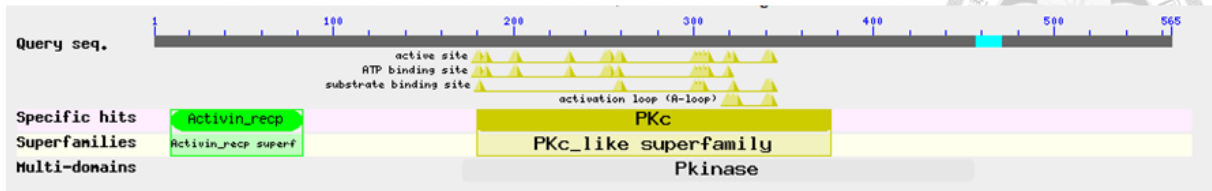
T GTG GAA CGT GCC AAT ATT ATA CCA CCT GTT CAG GAA TAT GGT GTA AAT AAC CTA AAT AAT GGA CAA G < 1632  
V E R A N I I P P V Q E Y G V N N L N N G Q V

TA TTT GAT GAT GTG GAG CTA ATG TCT GCT CCG CCA AAC GTG ATT CTT ATT AAC AAT GCA GTC GTA TGA < 1700  
F D D V E L M S A P P N V I L I N N A V V \*

TAG TAA CTA TAT CTG TTG ACT GCA GGT GAA GCC AGT GTG GCT AA < 1744



B



C

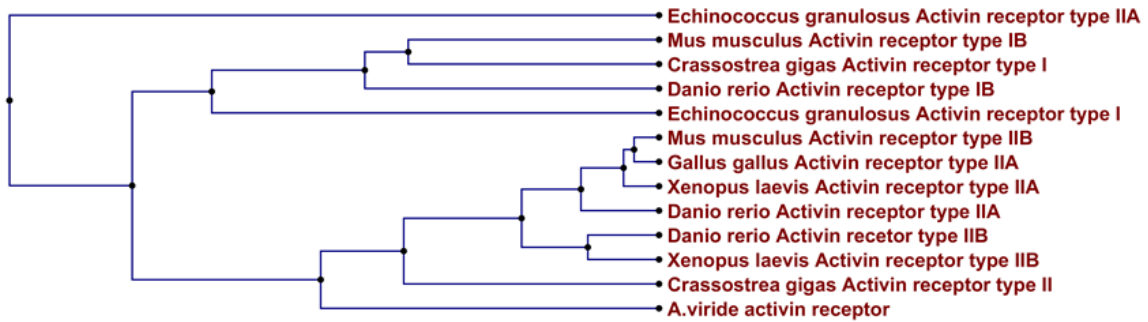
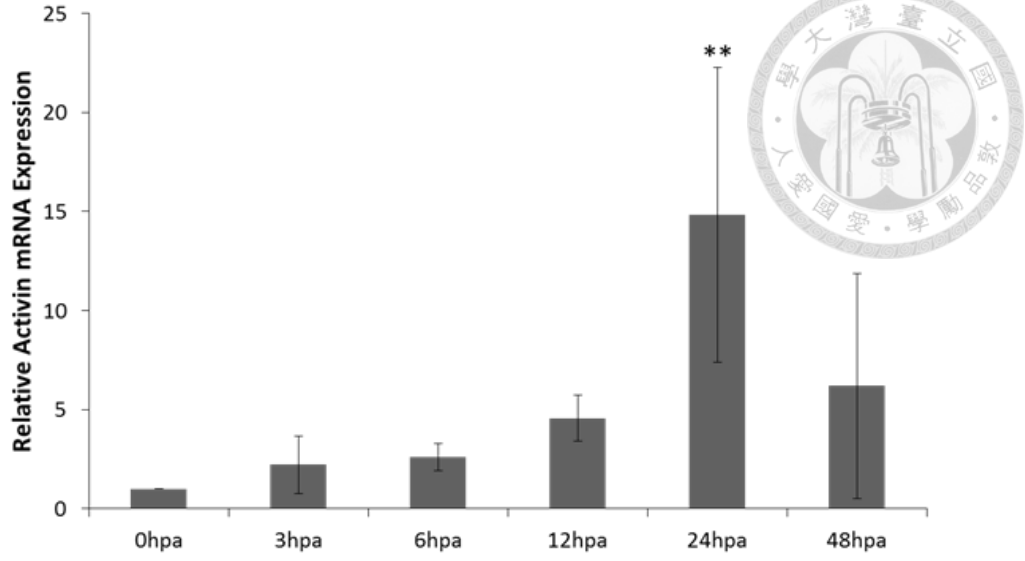
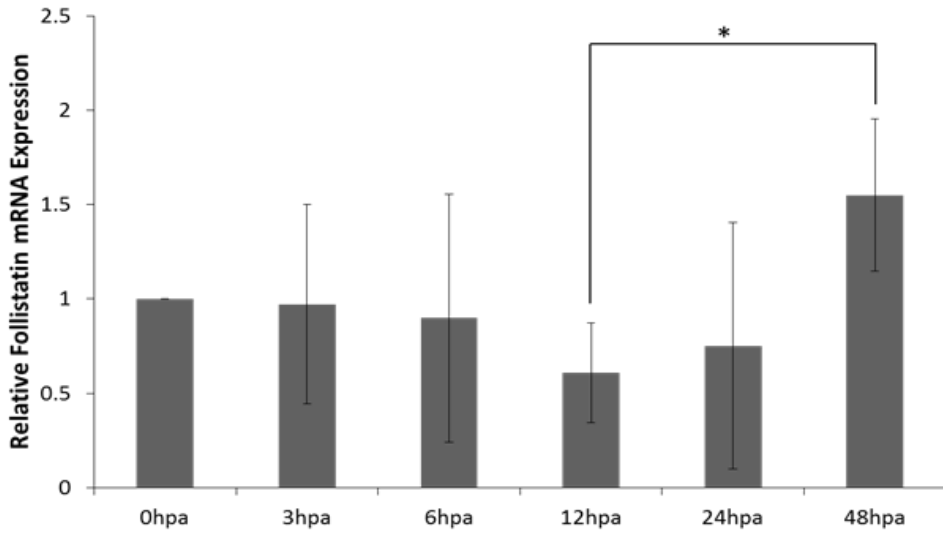


**Figure 4. Sequence of *Avi-activin receptor*.** (A) Partial mRNA sequence of *activin receptor*, about 1700 base pairs long, encodes a polypeptide of 565 amino acids with an Activin receptor conserved domain and protein kinase catalytic site indicating ATP binding activity (from NCBI) (B). (C) Comparing the protein sequence of activin receptor from *A. viride* to those from other species, its sequence is more similar to type II activin receptors. *Echinococcus granulosus*:dog tapeworm. *Crassostrea gigas*: Pacific oyster. *Mus musculus*: house mice. *Danio rerio*: zebrafish. *Gallus gallus*: chicken. *Xenopus laevis*: African clawed frog.

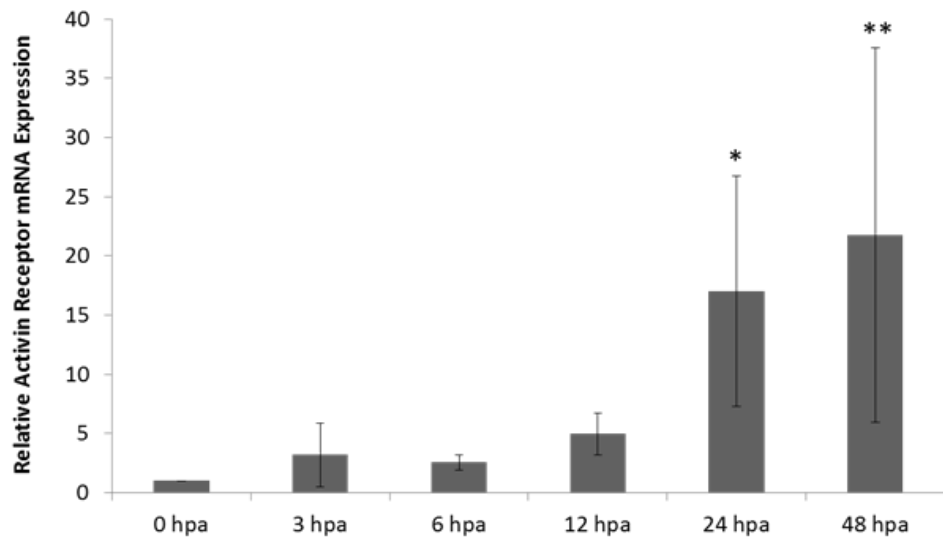
A



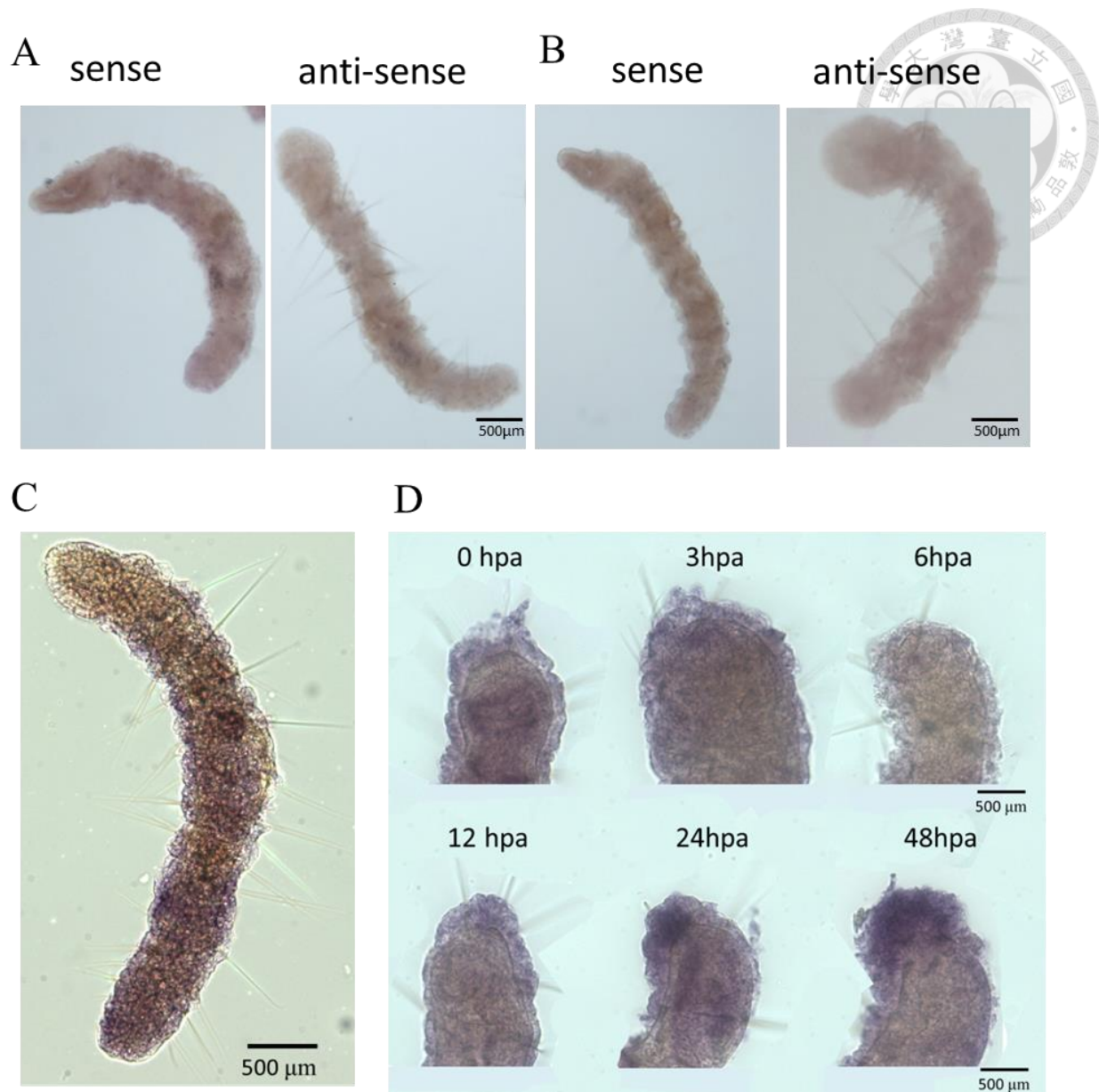
B



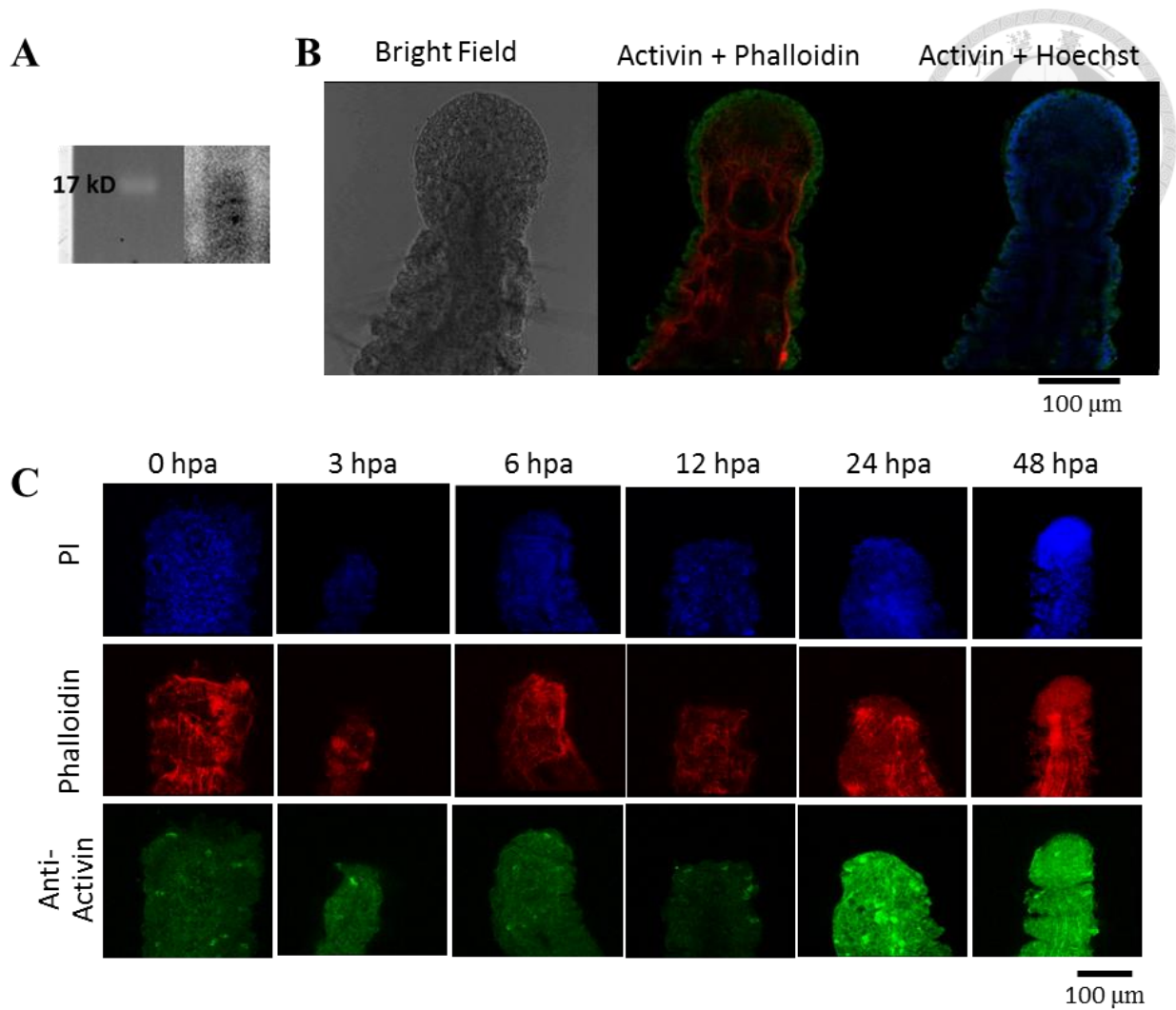
C



**Figure 5. Expression profiles of *Avi-activin*, *Avi-follistatin* and *Avi-activin receptor* during early regeneration.** Expression levels were normalized by house-keeping gene, actin, and plotted relative to 0 hpa. (A) *Avi-activin* expression increased after amputation, reached its peak at 24 hpa and dropped at 48 hpa. (B) Expression level of *Avi-follistatin* did not significant change in the period observed, except for a slight increase at 48 hpa. (C) Expression pattern of *Avi-activin receptor*, similar to that of *Avi-activin*, escalated after amputation, however, *Avi-activin receptor* continued to rise until 48 hpa. (\* $p < 0.05$ ; \*\* $p < 0.01$ )

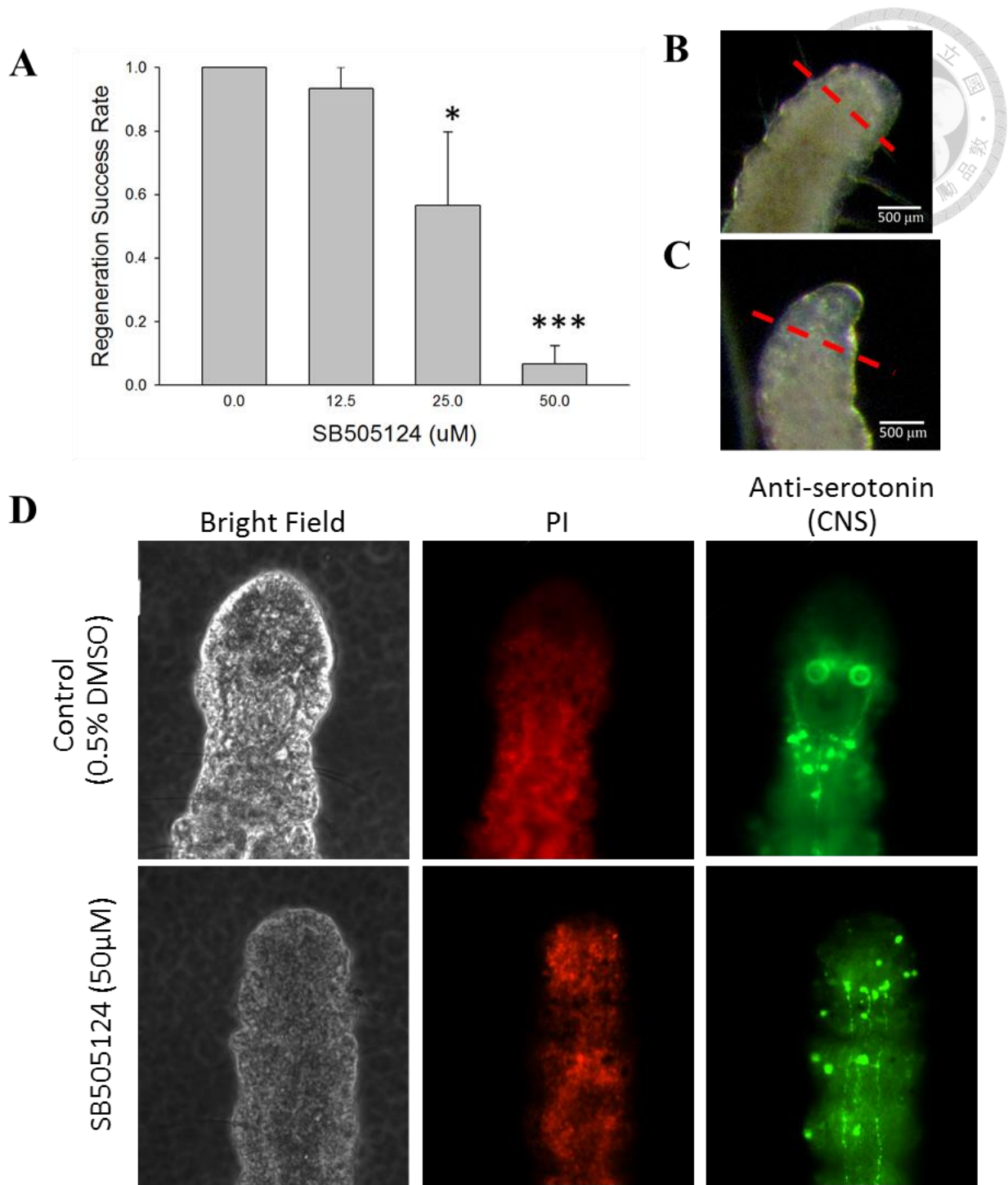


**Figure 6. Expression patterns of *Avi-activin*, *Avi-follistatin* and *Avi-activin receptor*.** In situ hybridization of *Avi-activin* (A) and *Avi-follistatin* (B) in intact *A. viride*. (C) *Avi-activin receptor* is expressed on the epithelium of intact worms. (D) During regeneration, *Avi-activin receptor* is expressed in the epithelium and concentrates in the regenerating tissue starting from 12 hpa and most obvious at 48 hpa.



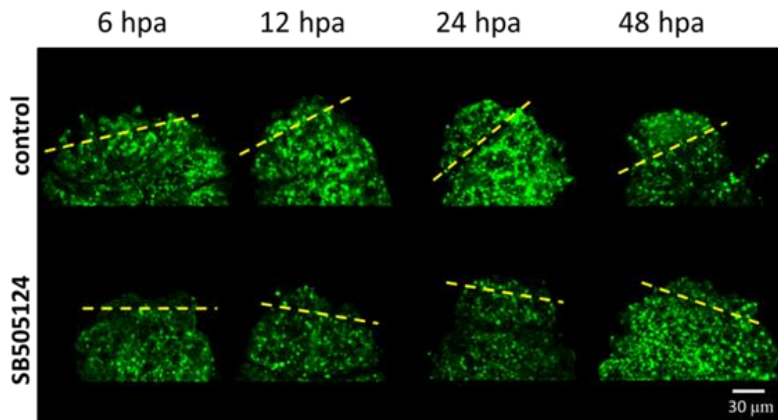
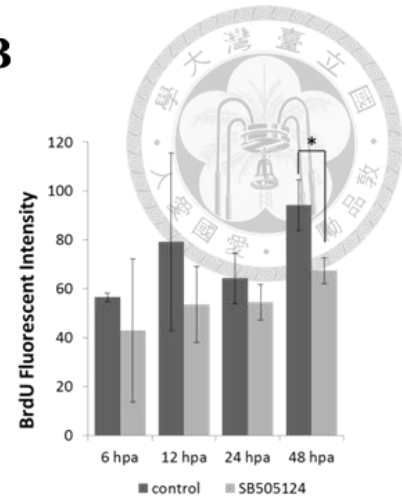
**Figure 7. Immunohistochemistry of Activin in intact and regenerating *A. viride*.** (A) Western blot of anti-Inhibin beta-A on total protein sample of intact *A. viride* shows a single band at about 15 kDa . Activin was expressed regularly in intact *A. viride* and throughout wound healing. (B) In intact *A. viride*, Activin surrounded the external margin of the organism, lining the external side of the muscle layer and overlaps with a layer of cell nuclei. (C) Throughout early regeneration, Activin is expressed on this layer of cells without obvious change in fluorescent intensity. Blue: Hoechst (cell nucleus), green: anti-Inhibin beta-A and red: Phalloidin (filamentous actin).





**Figure 8. Effects of SB-505124 treatment on the regeneration of *A. viride*.** (A) Amputated *A. viride* was treated with SB505124, an inhibitor of Activin/TGF- $\beta$  signaling. The results showed that inhibition of Activin/TGF- $\beta$  signaling affects anterior regeneration, resulting in two degrees

of defects (B and C). (B) Blastema formation is incomplete. (C) Blastema formation is complete with a tiny pharynx but head development is incomplete. (D) Control samples, treated with 0.5% DMSO, completed anterior regeneration. From the bright field view, the circular anterior structure and mouth opening located at the center are indicators of regeneration. The central nervous system, labelled by anti-serotonin, is composed of three vertical lines of nerves on the ventral side of the body, horizontally connecting before entering the prostomium and surrounds the mouth. SB505124-treated *A. viride* were unable to regenerate thus no protruding anterior structure or mouth opening is seen in the bright field view. Immunofluorescence of the central nervous system also indicates regeneration is incomplete, as the three vertical lines running down the body are not connected laterally in the anterior, nor do they extend into the new tissue or surround the mouth. Dashed line: amputation line. (\* $p < 0.05$ ; \*\*\* $p < 0.001$ )

**A****B**

**Figure 9. Cell proliferation in the regenerating tissue of *A. viride* with or without SB505124 treatment.** (A) Inhibition of Activin signaling affects cell proliferation at 48 hpa. Dashed line: amputation line. Green: anti-BrdU. (B) Quantification of fluorescent intensity in the blastmal region. ( $*p < 0.05$ )

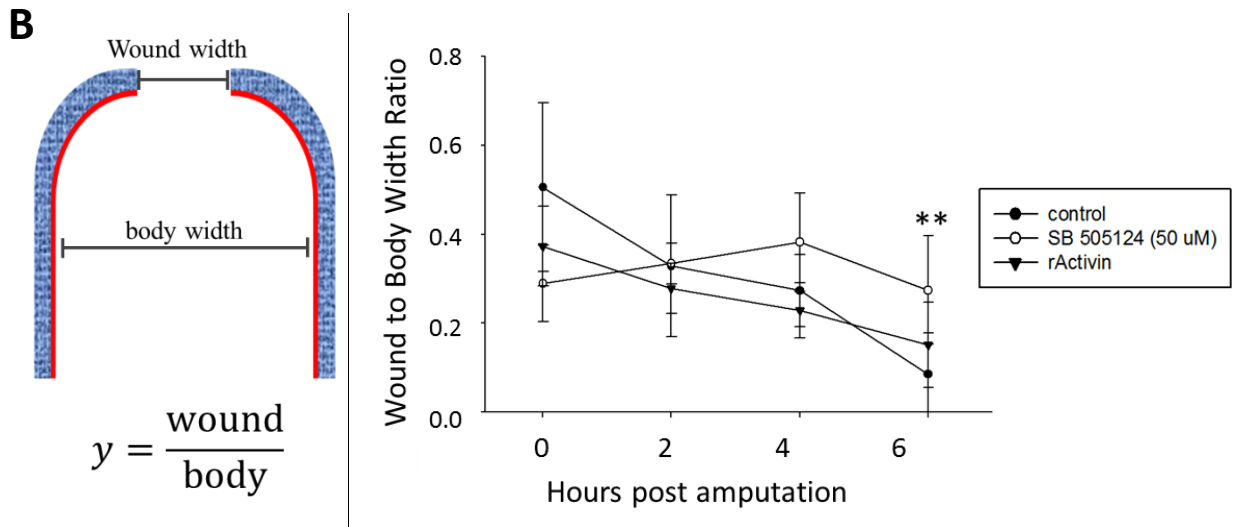
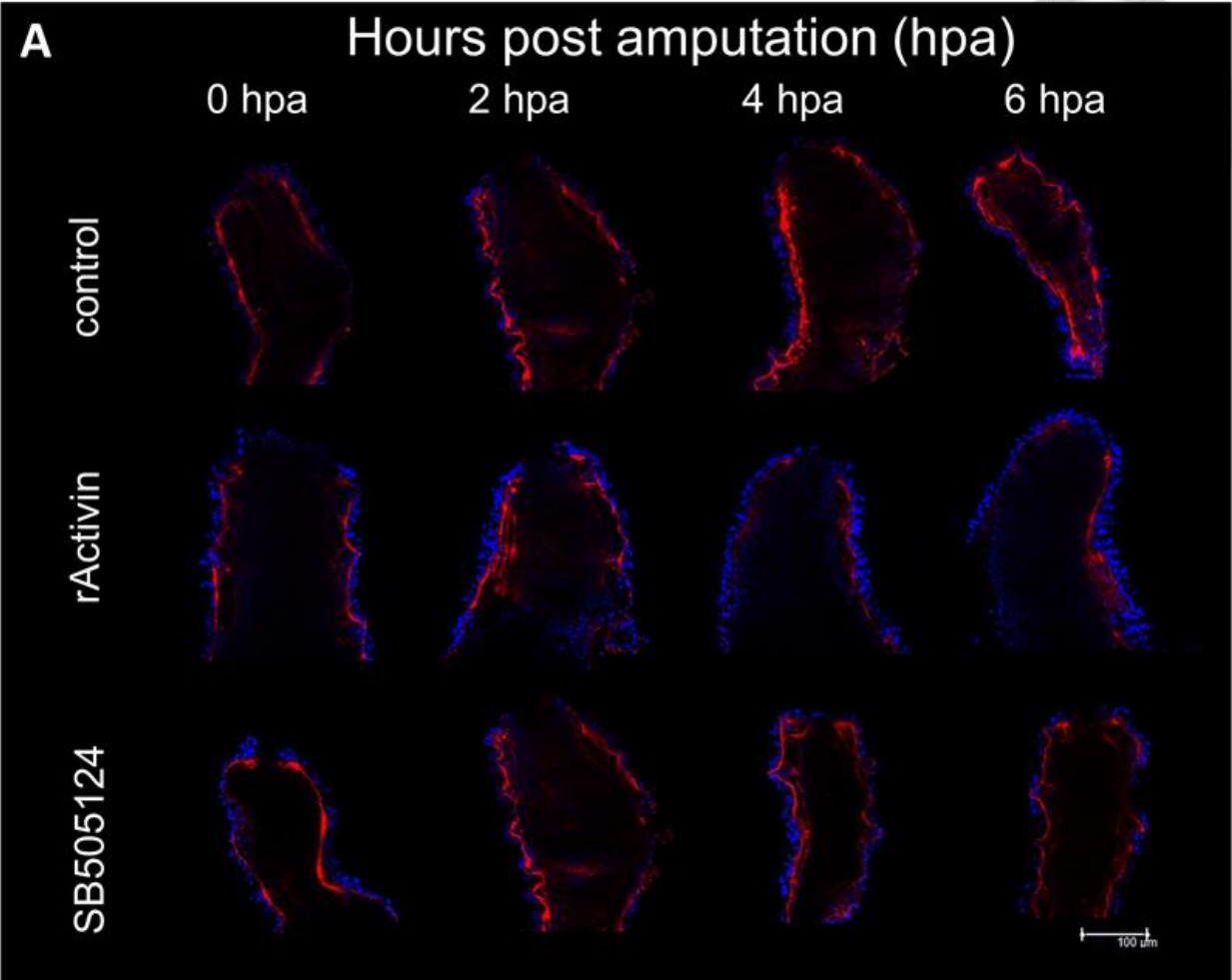


**Figure 10. Effects of SB505124 treatment on wound closure.** (A) Wound site of amputated *A. viride* stained with phalloidin and Hoechst. Blue: Hoechst (cell nucleus) and red: phalloidin (filamentous actin). (B) Quantification of wound size, shown on the left, was calculated as the ratio of wound width to body width, and then plotted against the corresponding time. The wound sizes of SB505124 treated *A. viride* were significantly larger than those of untreated individuals at 6 hpa. rActivin treatment showed no enhancement in wound closure. (\*\* $p < 0.01$ )

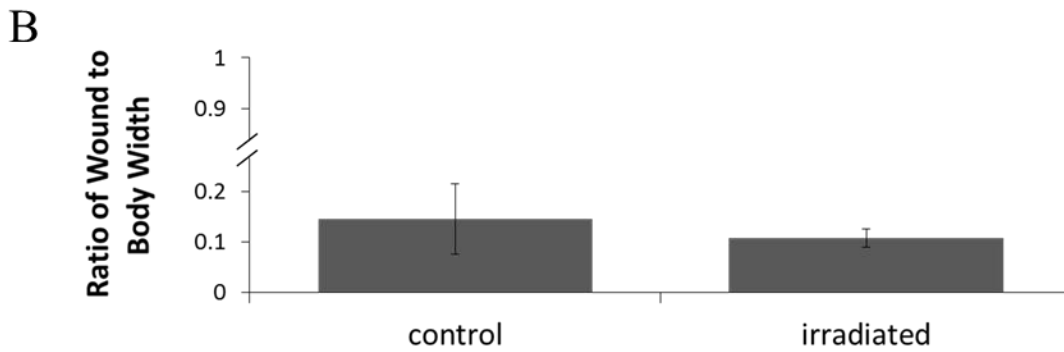
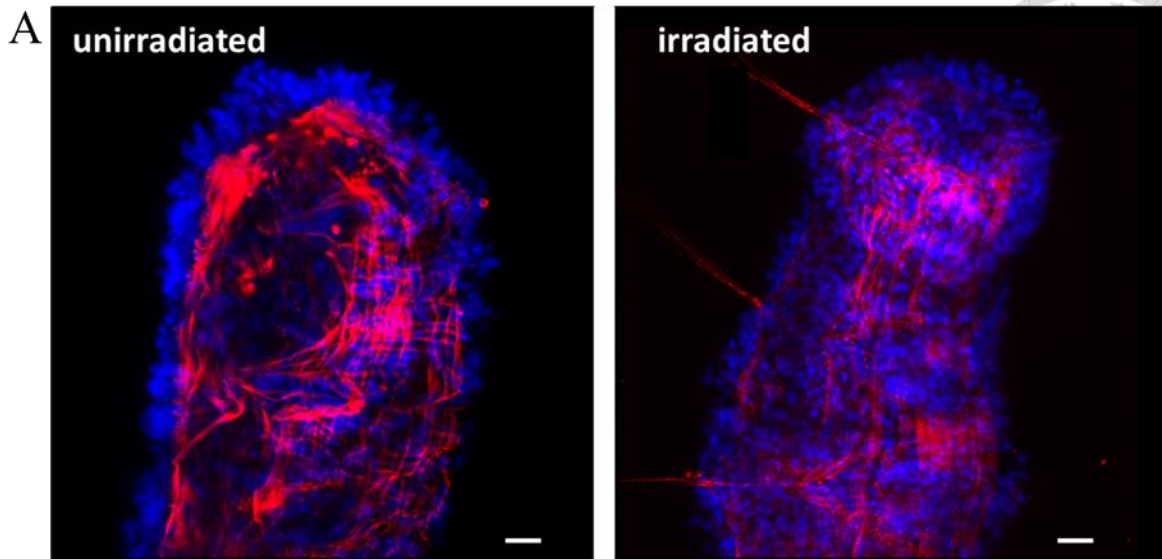


**Figure 11. Radiation effects on wound closure in *A. viride*.** (A) In comparison to unirradiated *A. viride*, irradiated individuals have lost proliferative ability but are capable of wound closure. (B) Quantification shows no significant difference between irradiated and unirradiated 6hpa wounds. Blue: Hoechst; Red: Phalloidin.